

GEAP-4566  
MARCH, 1964

Facsimile Price \$ 9.10

Microfilm Price \$ 3.50

Available from the  
Office of Technical Services  
Department of Commerce  
Washington 25, D. C.



MASTER

**EVESR**  
**NUCLEAR SUPERHEAT FUEL**  
**DEVELOPMENT PROJECT**  
**SEVENTH QUARTERLY REPORT**  
**DECEMBER 1963 - FEBRUARY 1964**

U.S. ATOMIC ENERGY COMMISSION  
CONTRACT AT(04-3)-189  
PROJECT AGREEMENT 29

ATOMIC POWER EQUIPMENT DEPARTMENT  
**GENERAL  ELECTRIC**  
SAN JOSE, CALIFORNIA

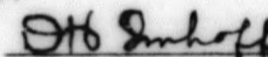
EVESR-NUCLEAR SUPERHEAT FUEL  
DEVELOPMENT PROJECT  
SEVENTH QUARTERLY REPORT  
DECEMBER - FEBRUARY 1964

Prepared by:



R. T. Pennington, Project Engineer  
ESADA-VESR Nuclear Superheat Fuel  
Development Project

Approved by:



D. H. Imhoff, Manager  
Engineering Development

U. S. Atomic Energy Commission  
Contract No. AT(04-3)-189  
Project Agreement 29

Printed in U. S. A. Price \$2. 25. Available from the  
Office of Technical Services, Department of Commerce,  
Washington 25, D. C.

ATOMIC POWER EQUIPMENT DEPARTMENT  
**GENERAL  ELECTRIC**  
SAN JOSE, CALIFORNIA

1726-TIO-2  
85-3/64

## LEGAL NOTICE

*This report was prepared as an account of Government sponsored work. Neither the United States, nor the Commission, nor any person acting on behalf of the Commission:*

- A. Makes any warranty or representation, expressed or implied, with respect to the accuracy, completeness, or usefulness of the information contained in this report, or that the use of any information, apparatus, method, or process disclosed in this report may not infringe privately owned rights; or*
- B. Assumes any liabilities with respect to the use of, or for damages resulting from the use of any information, apparatus, method, or process disclosed in this report.*

*As used in the above, "person acting on behalf of the Commission" includes any employee or contractor of the Commission, or employee of such contractor, to the extent that such employee or contractor of the Commission, or employee of such contractor prepares, disseminates, or provides access to, any information pursuant to his employment or contract with the Commission, or his employment with such contractor.*

CONTRIBUTORS

R. T. Pennington, Project Engineer  
EVE3R-Nuclear Superheat  
Fuel Development Project

S. Armour	W. V. Macnabb
D. L. Arndt	A. H. McQueen
B. G. Atraz	J. L. Murray
F. J. Brutschy	W. L. Pearl
F. A. Comprelli	H. P. Rebman
D. W. Danielson	T. A. Retter
D. L. Fischer	C. C. Ripley
M. D. Fitzsimmons	R. R. Roof
J. R. Fritz	M. Siegler
G. G. Gaul	R. H. Silletto
R. S. Gilbert	J. M. Skarpelos
V. E. Hazel	C. N. Spalaris
P. W. Ianni	W. A. Sutherland
L. T. Jones	H. T. Wells
A. R. Kimball	M. L. Weiss
E. A. Lees	N. D. Weiss

TABLE OF CONTENTS

<u>Section</u>		<u>Page</u>
1.0	INTRODUCTION AND SUMMARY	1-1
1.1	Introduction	1-1
1.2	Summary	1-2
2.0	SUB-TASK A-1: PROGRAM PLANNING AND EVALUATION	2-1
2.1	Critical Test Program	2-1
2.2	Prepower and Low Power Testing	2-2
2.3	Hydrogen and Oxygen Injection System	2-2
2.4	Turbine Tie-In	2-3
2.5	Installation of Fuel Evaluation Instrumentation	2-3
2.6	Installation of the Coolant Sampling System	2-4
3.0	SUB-TASK B-1: INITIAL FUEL DESIGN	3-1
4.0	SUB-TASK B-2: INITIAL FUEL DESIGN - ENGINEERING PHYSICS	4-1
4.1	Hazards Evaluations	4-1
5.0	SUB-TASK C-1: INITIAL FUEL FABRICATION	5-1
6.0	SUB-TASK C-2: INITIAL FUEL ELEMENT DEVELOPMENT AND FABRICATION	6-1
7.0	SUB-TASK C-3: NEUTRON SOURCE PREPARATION	7-1
8.0	SUB-TASK C-4: FUEL EVALUATION INSTRUMENTATION	8-1
8.1	Testing	8-1
8.2	Instruction Manuals	8-1
8.3	Moderator Flow Instrumentation	8-1
9.0	SUB-TASK C-5: FUEL CHEMISTRY EVALUATION INSTRUMENTATION	9-1
9.1	Coolant Sampling System Instrumentation	9-1
9.2	Oxygen and Hydrogen Gas Analyzer	9-1
9.3	Crud Concentrator	9-2
10.0	SUB-TASK D-1: ENGINEERING PHYSICS	10-1
10.1	Summary	10-1
10.2	Description of Critical Measurements	10-1
11.0	SUB-TASK D-2: TEST ENGINEERING	11-1
12.0	SUB-TASK D-3: TEST SPECIFICATIONS	12-1

TABLE OF CONTENTS (Continued)

<u>Section</u>		<u>Page</u>
13.0	SUB-TASK D-4: DATA PROCESSING	13-1
14.0	SUB-TASK D-5: COOLANT CHEMISTRY AND FUEL ACTIVITY RELEASE	14-1
	14.1 Specifications and Data Requirements	14-1
	14.2 Sampling and Procedures	14-1
	14.3 Boiler Water Chemistry	14-1
	14.4 Moderator Water Chemistry	14-2
	14.5 Condensate Demineralizer Effluent Chemistry	14-2
	14.6 Hotwell Water Chemistry	14-3
	14.7 Chemistry of Other Streams	14-3
15.0	SUB-TASKS E-1 AND E-2: FUEL EXAMINATIONS	15-1
16.0	TASK F: NUCLEAR SUPERHEAT FUEL DEVELOPMENT PROGRAM	16-1
	16.1 Objectives	16-1
17.0	SUB-TASK F-1: ADVANCED FUEL, GENERAL DEVELOPMENT	17-1
	17.1 High Temperature Autoclave Testing of Fuel Capsules	17-1
	17.2 Heat Transfer Tests	17-1
	17.3 Stress Corrosion Cracking of Superheat Fuel Sheating	17-2
	17.4 Fuel Clad Strain Cycling	17-9
	17.5 NTR Test of EVESR Cladding Materials	17-14
	17.6 Heat Transfer Analytical Analysis	17-15
18.0	SUB-TASK F-2: FUEL FABRICATION	18-1
	18.1 Fuel Bundle Material Procurement - Mark III	18-1
	18.2 Incoming Tubing Inspections	18-1
19.0	SUB-TASK F-3: MARK III FUEL DESIGN	19-1
	19.1 Physics	19-1
	19.2 Heat Transfer and Design Analysis	19-2
	19.3 Fuel Bundle Design	19-3
	19.4 Bundle Tooling Design and Fabrication	19-4
	19.5 Steam Flow Tests on Advanced Fuel Components	19-4
	19.6 Mark III Fuel Element Design	19-4
	19.7 Fuel Element Fabrication Development	19-4
	REFERENCES	1
	DISTRIBUTION	3

LIST OF ILLUSTRATIONS

<u>Figure</u>	<u>Title</u>	<u>Page</u>
3-1	Initial Arrangement of Mark II Fuel in the EVESR Core, Showing Planned Operating Conditions at 12.5 MW Based on DARE Calculations	3-2
8-1	Flowmeter	8-3
8-1 a	Flowmeter Parts List	8-5
10-1	EVESR, Mk II Core, Multiplication Versus Moderator Temperature	10-4
10-2	EVESR Minimum Unflooded Critical, November 26, 1963	10-5
13-1	EVESR Mark II Fuel Operating Parameters	13-2
13-2	EVESR Mark II Fuel Operating Parameters	13-3
13-3	EVESR Mark II Fuel Operating Parameters	13-4
13-4	EVESR Mark II Fuel Operating Parameters	13-5
13-5	EVESR Mark II Fuel Operating Parameters	13-6
17-1	Tensile Specimen For Stress Corrosion Tests (~ 1.3X)	17-7
17-2	Corrosion Test in Progress. Solution is Boiling 42 w/o MgCl <sub>2</sub>	17-8
17-3	Stress Versus Time-To-Failure in Boiling 42 Weight Percent MgCl <sub>2</sub>	17-10
17-4	Macrograph of 310 VM Stainless Steel Test Specimen and Micrograph Showing Stress Corrosion Cracks	17-11
19-1	EVESR Fuel Rod	19-5
19-2	EVESR Mark III Fuel Cluster	19-7
19-3	Cross Section of EVESR Mark III Fuel	19-10

## 1.0 INTRODUCTION AND SUMMARY

### 1.1 Introduction

This is the seventh in the series of quarterly progress reports being issued to cover the work performed on the EVESR-AEC Nuclear Superheat Fuel Development Project under Contract AT(04-3)-189, P. A. 29. The EVESR plant design and the design of the first core load of fuel are described in detail in GEAP-4105, "The First Quarterly Report," and in APED-3958, "Final Hazards Summary Report for the ESADA-VESR." The seventh quarterly report is intended to cover the technical progress on the AEC-sponsored EVESR Nuclear Superheat Fuel Development Project for the period between December 1, 1963 and February 29, 1964.

#### Nuclear Superheat Fuel Development Program Reports Issued to Date

##### Quarterly Reports

- First - May 1962 through August 1962, GEAP-4105
- Second - September through November 1962, GEAP-4146
- Third - December 1962 through February 1963, GEAP-4200
- Fourth - March through May 1963, GEAP-4277
- Fifth - June through August 1963, GEAP-4363
- Sixth - September through November 1963, GEAP-4432
- Seventh - December 1963 through February 1964, GEAP-4566

##### Topical Reports

- "Physics Pre-Startup Report," April 1963, GEAP-4213

The EVESR-AEC Nuclear Superheat Fuel Development Project has been organized into the following work task areas:

- Sub-task A-1: Program Planning and Evaluation;
- Sub-task B-1: Initial Fuel Design;
- Sub-task B-2: Initial Fuel Design, Engineering Physics;
- Sub-task C-1: Initial Fuel Fabrication;
- Sub-task C-2: Initial Fuel Element Development and Fabrication;
- Sub-task C-3: Neutron Source Preparation;
- Sub-task C-4: Fuel Evaluation Instrumentation;
- Sub-task C-5: Fuel Chemistry Evaluation Instrumentation;
- Sub-task D-1: Fuel Tests, Engineering Physics;
- Sub-task D-2: Fuel Tests, Test Engineering
- Sub-task D-3: Fuel Tests, Test Specifications;



- Sub-task D-4: Fuel Tests, Data Processing;
- Sub-task D-5: Fuel Tests, Activity Release and Coolant Chemistry;
- Sub-task E-1: Fuel Examination Planning and Evaluation;
- Sub-task E-2: Fuel Pre- and Post-Irradiation Examinations
- Sub-task F-1: Advanced Fuel General Development;
- Sub-task F-2: Advanced Fuel Fabrication;
- Sub-task F-3: Mark III Fuel Design and Development; and
- Sub-task F-4: Mark IV Fuel Design and Development.

These tasks will serve as a basic outline for the reporting of progress in this and future quarterly progress reports.

## 1.2 Summary

1. Criticality with the full core loading of 32 fuel bundles was first achieved on December 3, 1963.
2. The critical test program, consisting of making physics measurements with the reactor in the following conditions, was completed in February 1964:
  - a. Cold, steam passages unflooded;
  - b. Cold, steam passages flooded;
  - c. Hot, steam passages flooded; and
  - d. Hot, steam passages unflooded.

The results of the critical test program are reported under Sub-tasks A-1 and D-1.

3. Detailed test procedures have been prepared for the prepower and power tests which are expected to be conducted during the next quarter.
4. Plans and specifications for the Oxygen and Hydrogen Injection System are completed, and procurement bids are being received.
5. The installation of the Fuel Evaluation Instrumentation System was completed with the placing and connection of the R and D Instrument Panel in the Control Room. The first phase of tests to assure the proper operation of this instrument system has been successfully completed. Details of these activities are reported under Sub-tasks A-1 and C-4.
6. The installation of the Coolant Sampling System is complete, and reactor operating personnel are being trained in the techniques of taking steam samples and operating the instruments.

7. Specifications calling out the specific limits of temperature, power level, and coolant chemistry conditions to be maintained on the Mark II fuel have been prepared.
8. The DARE program for computer computation of EVESR fuel operating conditions has been completed (option 5) to allow the generation of operating curves. These curves show the relationships among the following key reactor and fuel operating parameters:
  - a. Fuel clad surface temperature,
  - b. Steam coolant flow rate,
  - c. Reactor power level, and
  - d. Superheated steam exit temperature.

These curves are shown under Sub-task D-4.

9. A preliminary plan for the advanced fuel program has been developed and is presented under Task F.
10. The layout design of Mark III fuel bundle has been completed and approximately 90 percent of the material required for fabrication has been ordered. Tubing for fuel element cladding has been ordered and is being received and inspected.

## 2.0 SUB-TASK A-1: PROGRAM PLANNING AND EVALUATION

### 2.1 Critical Test Program

Activities at the EVESR site during December, January, and February centered around completing the loading of the 32 Mark II fuel bundles and conducting the planned critical test program.

Criticality with the full core loading of 32 fuel bundles was first achieved on December 3, 1963, and critical testing with the core in the cold, unflooded condition was completed. The results were reviewed with members of the AEC Division of Licensing and Regulation and concurrence was obtained to proceed with the next phase of critical tests with the core in the flooded condition.

The unflooded core was unloaded to eight bundles and the core was flooded. Fuel bundles were then reloaded and criticality in the cold, flooded condition was achieved on December 20, 1963, with 14 fuel bundles in the core. Loading of the remaining fuel bundles was completed on December 26, 1963, and critical testing resumed with the full core of 32 fuel bundles in the cold, flooded condition.

Cold critical testing of EVESR was completed during January. These tests included measurements of the temperature coefficient up to 180°F and control rod worth measurements for the flooded core.

Preliminary results of the cold critical test program were reviewed with the AEC Division of Licensing and Regulation on January 3, and it was agreed at that time to proceed with the hot critical tests, including the tests which required installation of the superheated steam jumper pipes.

Following completion of the cold tests, one of the four permanent antimony-beryllium sources was installed in the core and the out-of-core nuclear instruments were calibrated against the in-core detectors used during the earlier phases of the test. All 32 of the superheat steam jumper pipes were installed for the first time.

The hot critical tests were initiated on January 17. These tests included measurement of the temperature coefficient from 300°F to 545°F with the fuel both flooded and unflooded. Control rod worths were evaluated at operating conditions using normal period techniques.

The critical test program was completed during February. The final tests performed emphasized measurement of critical physics parameters with the reactor at elevated temperatures and with the fuel steam passages unflooded. In addition, special measurements were performed to determine the worth of individual control rods with various rod configurations at several intermediate moderator temperatures. Most of the measurements were made using

period techniques. However, these results were supplemented by use of the pulsed neutron source at temperatures up to 375 F. The pulsed neutron equipment was used successfully during three phases of the test program and provided useful information which would have been otherwise unavailable.

Detailed results of the critical test program are presented under Sub-task D-1.

## 2.2 Prepower and Low Power Testing

Following the critical test program, the series of prepower and low power tests listed below will be conducted. Detailed test procedures have been prepared based on the test outlines which were completed previously:

- a. Flow nozzle calibration;
- b. Plant flow (This test has been completed);
- c. Unflooding (This test has been completed);
- d. Flow distribution;
- e. Emergency cooling;
- f. Heat balance calibration;
- g. Core temperatures;
- h. Reactor water level;
- i. Pressure controller;
- j. Outlet flow controller;
- k. Control rod run-in and run-out;
- l. Simulated cold water accident and moderator recirculation;
- m. Flux, flow, and temperature computer;
- n. Clean up flow transient;
- o. Scram without isolation;
- p. Pressure oscillation;
- q. Plant radiation;
- r. Off-gas system calibration;
- s. Fuel evaluation instrumentation;
- t. Control of bias flow control valves (completed); and
- u. Pipe gallery cooling.

Special instrumentation, such as high speed recorders required for the prepower and power tests, has been assembled and installed.

## 2.3 Hydrogen and Oxygen Injection System

Plans and specifications for a Hydrogen and Oxygen Injection System have been completed. This system will inject hydrogen and oxygen gas into the saturated steam header at a point between the boiler and the reactor. The purpose of the system is to simulate the radiolytic

gas content of typical steam from boiling water reactors. The flow of hydrogen and oxygen from gas storage bottles will be controlled in such a manner that the stoichiometric gas fractions of 20 ppm oxygen and 2.5 ppm hydrogen will be present in the steam reaching the reactor. The operation and control of the gas injection system will be automatic. In addition, a gas analysis instrument is being designed which will measure and produce an independent record of the actual gas content of the steam downstream of the injection point. The gas analysis instrument is described under Sub-task C-5.

#### 2.4 Turbine Tie-In

Design and procurement work was initiated on an interconnection between the EVESR superheat steam header and the existing VBWR turbine. This connection will permit the EVESR steam to be utilized in the turbine which was previously operated with steam from the VBWR.

#### 2.5 Installation of Fuel Evaluation Instrumentation

The R and D Instrument Panel was installed in the EVESR control room in December, and the electric cable connections were made to the sensors and signal transmitters. The sensors and signals transmitters, located in the reactor containment building, were installed previously.

The EVESR Fuel Evaluation Instrument System, which was described in detail in the Fifth Quarterly Report, GEAP-4363, has been installed to fulfill the following requirements of the nuclear superheat fuel development program:

- a. To measure and record the temperature, pressure, and flow rate of the superheated steam from each of the 32 fuel bundles that make up the reactor core. These variables are measured in the 32 steam exit lines just outside the reactor pressure vessel.
- b. To indicate and alarm when any fuel bundle is operating at high or low temperatures, as evidenced by the steam temperatures.
- c. To provide a means of adjusting the bundle steam flow control valves for the purpose of controlling the fuel operating temperature.
- d. To measure and record approximately 20 coolant and moderator temperatures at selected points within each of the eight instrumented fuel bundles in the "south" quarter section of the reactor core.
- e. To provide a central instrument read-out point for fuel evaluation instrumentation for both the initial (Mark II) fuel and for additional instruments which may be applied to the advanced fuel.

Following installation, tests were conducted on the Fuel Evaluation Instrument System. These tests are described under Sub-task C-4.

#### 2.6 Installation of the Coolant Sampling System

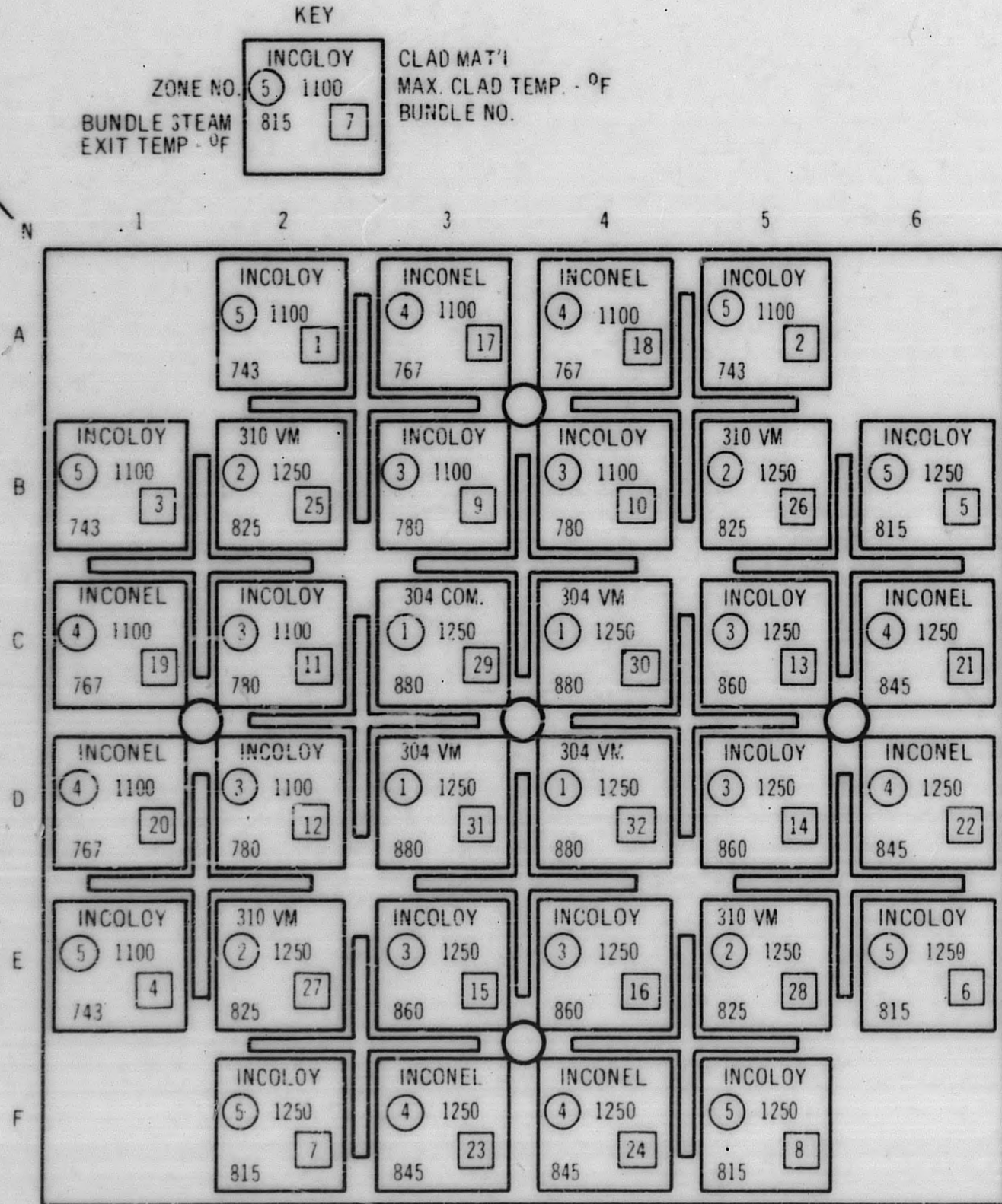
Installation of the basic coolant sampling system is complete and Operations personnel are being trained in the techniques of taking samples and operating the instruments. Tests on the accuracy of the automatic chloride analyzer are being conducted prior to its release for regular use by Operations personnel.

### 3.0 SUB-TASK B-1: INITIAL FUEL DESIGN

The design and fabrication of the initial (Mark II) EVESR fuel is complete. The design is described in the Fifth Quarterly Report, GEAP-4363.

The present status of the 37 Mark II fuel bundles is as follows:

- |  |   |
|--|---|
| Bundles 1 through 32:                  | Loaded in the reactor as shown in Figure 3-1.                                     |
| Spare Bundle 33 (Incoloy clad - SPL1): | Being adapted for moderator flow measurement as reported under Sub-task C-4.      |
| Spare Bundle 34 (Incoloy clad - SPL2): | Instrumented and used for controlled steam passage flooding and unflooding tests. |
| Spare Bundle 35 (Inconel clad - SPM1): | Available as a spare.   |
| Spare Bundle 36 (Inconel clad - SPM2): | Available as a spare.   |
| Spare Bundle 37 (Inconel clad - F3M):  | Contains fuel element clad thermocouples. Available for insertion.                |



1726-7

Figure 3-1. Initial Arrangement of Mark II Fuel in the EVESR Core, Showing Planned Operating Conditions at 12.5 MW Based on DARE Calculations



#### 4.0 SUB-TASK B-2: INITIAL FUEL DESIGN - ENGINEERING PHYSICS

##### 4.1 Hazards Evaluations

Hazards studies related to the EVESR reactor have been extended to take into consideration any changes to previously assumed nuclear characteristics resulting from the critical test program. Of particular importance in this respect were the measurements of control system strength and partial unflooding reactivity effects. The measurements indicated that the strength of the outer control blades relative to the inner control blades was less than had been predicted in the initial design calculations. Despite the fact that the total control system was found to be essentially as calculated for the Final Hazards Summary Report (FHSR),<sup>(1)</sup> the maximum strength of a single blade was found to be somewhat greater than had previously been assumed. The maximum strength blade was found to be one of the four central, stainless steel control blades. Calculations were made to investigate the transients resulting from the drop-out of a maximum strength control blade in both the cold flooded reactor and the hot unflooded reactor.

Two compensating changes have occurred which leave the calculated effects of hot control rod drop-out accidents essentially unchanged from that described in the FHSR. The hot control rod drop-out accidents summarized in the FHSR utilized the Doppler reactivity coefficient, shown on FSHR Figure II.C.5, for a moderator temperature of 68°F. The more appropriate Doppler coefficients for these cases is the curve, shown also on Figure II.C.5, for a moderator temperature of 545°F. Applying this more appropriate coefficient results in greater Doppler control than previously calculated which compensates for the increase in maximum hot rod worths in both normal and abnormal patterns. Thus, the increase in maximum normal pattern rod worth from 0.016  $\Delta k$  to 0.021  $\Delta k$  still results in an accident which does not exceed the core destruction threshold. The increase in maximum abnormal pattern rod worth from 0.033  $\Delta k$  to 0.037  $\Delta k$  still results in an accident of approximately 2300 MW-seconds of energy production and fuel rupture in approximately 19 percent of the core volume as described in Section IV.C.4 of the FHSR.

The worst cold drop-out accident is described in Section IV.G.3 of the FHSR. This accident was calculated to result in 2350 MW-seconds of energy produced and destruction of approximately 17 percent of the core on the basis of a cold rod worth of 0.019  $\Delta k$ , 1 dollar of unflooding reactivity available, and a 50-cent contribution from the positive moderator temperature coefficient. On the basis of the current maximum abnormal pattern cold rod worth of 0.03  $\Delta k$ , and 2.4 dollars of available unflooding reactivity, in addition to the positive temperature coefficient effect, the accident is now calculated to produce 2550 MW-seconds of energy and to result in approximately 20 percent core destruction. While the effects of this accident are now increased slightly compared to the previous results, this increase of a few percent in core destruction is not considered significant.

Additional studies have been completed to increase our understanding of the time dependence of reactivity additions resulting from unflooding in the unlikely event of a nuclear heatup accident. (The reactor is normally heated by steam from an external gas-fired boiler.) The most important result of this work was the fact that unflooding of the inner superheat pass either precedes or is concurrent with unflooding the outer superheat pass. This implies that the more positive reactivity gain associated with unflooding only the outer superheat pass will not be seen in a nuclear heatup accident.

In addition, previous analyses had assumed that 50 percent of the water was expelled during the first Btu/lb enthalpy rise in the water. The remaining water was then expelled as sufficient energy was supplied to boil it off. More detailed thermal hydraulic analyses have shown that under most circumstances considerably more than 1 Btu/lb is required to void the first half of the water. However, considerably less time is involved in voiding the second half. The net result has been a trend to increase the available unflooding reactivity in relatively slow nuclear heatups, and to slightly decrease the available reactivity during fast heatups resulting from rapid reactivity insertions. The net effect seems to indicate that the relatively simple unflooding model employed in the hazards analysis is a reasonable first order estimate.

#### 5.0 SUB-TASK C-1: INITIAL FUEL FABRICATION

The fabrication of the 37 bundles of initial (Mark II) fuel is complete. The fabrication processes for the Mark II fuel were described in the Fifth Quarterly Report, GEAP-4363. This completes the work under this task.

**6.0 SUB-TASK C-2: INITIAL FUEL ELEMENT DEVELOPMENT AND FABRICATION**

Development and fabrication of the initial (Mark II) fuel elements (annular rods) for EVESR has been completed. This completes the work under this task.

### 7.0 SUB-TASK C-3: NEUTRON SOURCE PREPARATION

The antimony rods for the neutron sources were rechecked for curie content and compared with those readings reported last quarter, with the following results:

Source Number	Curies Sb-124	
	<u>±20 Percent</u> <u>October 22, 1963</u>	<u>±10 Percent</u> <u>January 2, 1964</u>
1	1400	635
2	1650	736
3	1375	621
4	1650	714

These results fall reasonably close to the theoretical decay curve.

One source rod was shipped to EVESR on January 3, 1964, for insertion in the reactor. The remaining three are being stored at the Vallecitos Radioactive Materials Laboratory pool until they are needed at EVESR late in February 1964.

## 8.0 SUB-TASK C-4: FUEL EVALUATION INSTRUMENTATION

### 8.1 Testing

Following completion of the installation of the R and D Instrument Panel in the control room and connection of the electric cables to the reactor containment building, two phases of testing were scheduled for the Fuel Evaluation Instrumentation System. The first phase consisted of simultaneously applying simulated steam temperature, pressure, and flow signals to the transducers and transmitters in the control room, and observing the readout on the R and D Instrument Panel. The purpose of this test was to verify all the electrical connections and calibrations made previously, and to check the proper operation of the corrected mass flow computer which is located in the R and D Instrument Panel. This test was completed in February; all components functioned as planned and were within tolerance. Steam flow bias control valve operation and indication on the R and D Instrument Panel was also checked and found to be satisfactory.

The second phase of tests to be conducted on the Fuel Evaluation Instrument System consists of verifying the actual steam temperature, pressure, and flow readings on the R and D Instrument Panel when the reactor plant is at operating conditions. These tests are expected to be performed in March.

### 8.2 Instruction Manuals

The instruction manual for the Fuel Evaluation Instrument System is being completed. Volume III, a collection of the equipment vendors' manuals, has been issued in final form. Volume II, an assembly of the as-built engineering drawings for the System, has been issued in draft form. Volume I, a complete engineering description of the Instrument System, is being drafted.

### 8.3 Moderator Flow Instrumentation

Spare Mark II fuel bundle SPL2 is in the process of being modified in the fuel shop to incorporate a turbine-type flowmeter for measuring the moderator flow rate past the process tube. The functions of this instrument was described in the Sixth Quarterly Report, GEAP-4432. It is shown in Figure 8-1 how the flowmeter is installed on the nose of the SPL1 fuel bundle. The fuel channel is shown in phantom. Part 1 is the nose piece of the fuel bundle; it is cut off and the flowmeter assembly is welded to the nose piece. The pickup coil, part 11, is held in position by a spring to insure that the coil is properly seated. The pickup coil is an electromagnet which is positioned inside of the rotor. The rotor has a twelve-fingered armature of high permeable material. As the rotor turns the magnetic reluctance changes; this will induce twelve pulses per revolution of the rotor. The readout instrumentation converts this signal into an analog signal that is proportional to the pulse frequency. The end of the pickup coil case has a stellite pad which is the thrust bearing for the rotor. The meter, part 4, is mounted on the basic assembly with the flange, part 6. The seal, part 3, is positioned by four corner springs, part 7, to insure that all the moderator flow goes through the meter.

798D941

2

3

4

5

6

7

8

9

GENERAL ELECTRIC

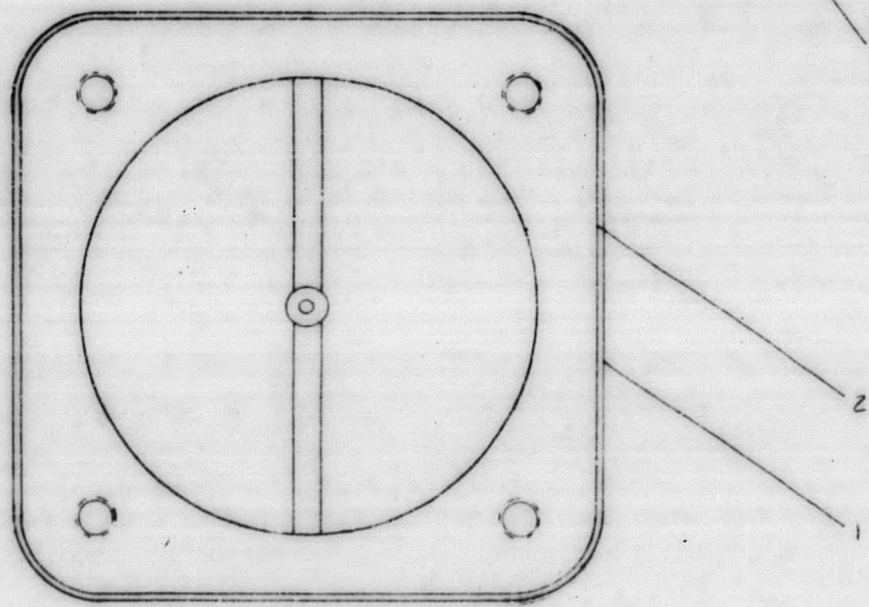
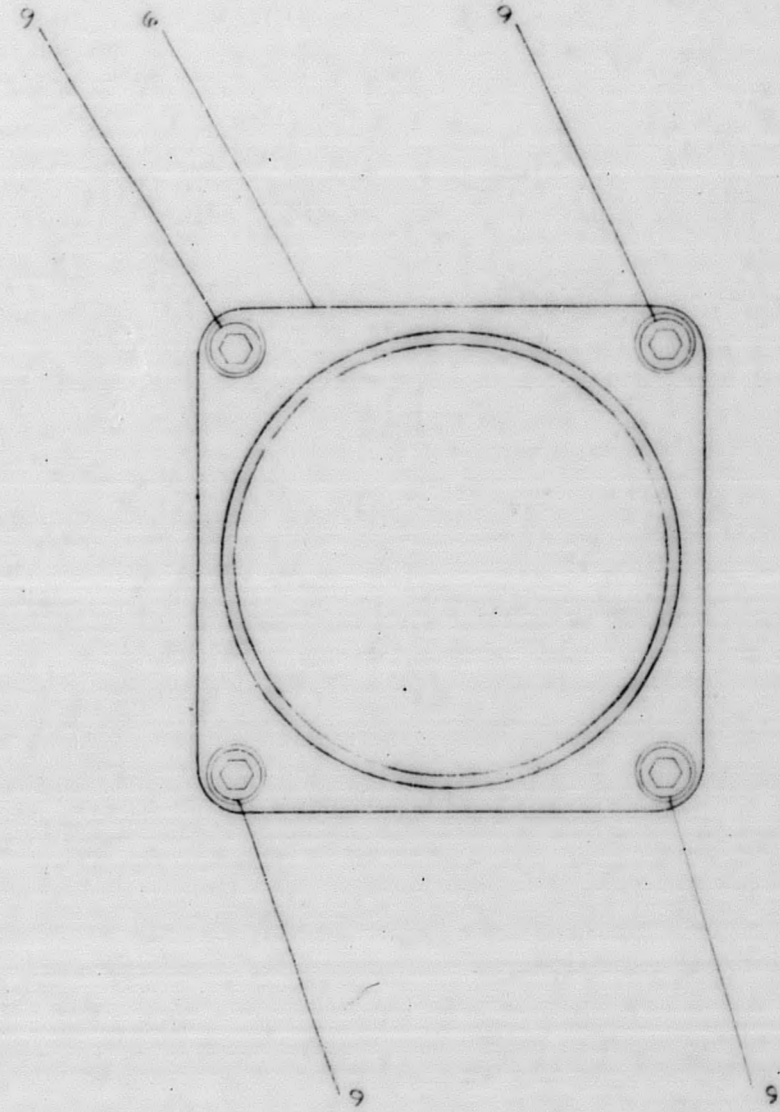
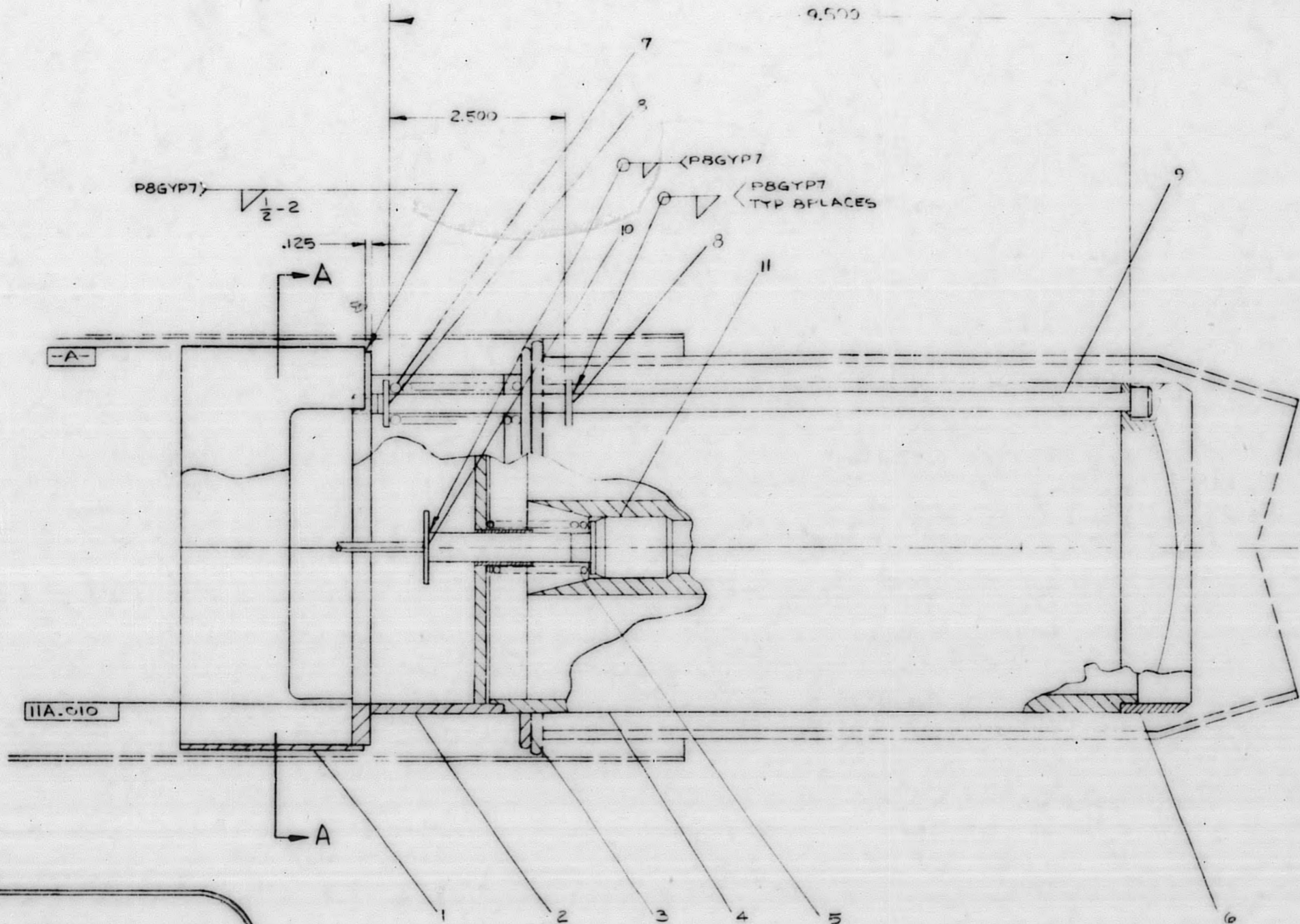
GEAP-4566

798D941

UNLESS OTHERWISE SPECIFIED USE THE FOLLOWING			
APPLIED PRACTICES	SURFACES	TOLERANCES UNLESS OTHERWISE SPECIFIED	ANGLES
145A5481	✓	0.01	

TITLE AEM  
**FLOW METER**  
 FIRST MADE FOR VESR

PL ISSUED FCF 212 E625



SECTION A-A

APPROVALS	INITIAL	DATE
MAT'L ENGR		2 10 64
ENGR DEVL	JFS	2/1/64

DESCRIPTION OF GROUPS	REVISIONS	PRINTS TO

10 DEC 63  
 798D941  
 APED  
 SANDOSE  
 798D941  
 INEPS

8-3/8-4

Figure 8-1. Flowmeter





## 9.0 SUB-TASK C-5: FUEL CHEMISTRY EVALUATION INSTRUMENTATION

### 9.1 Coolant Sampling System Instrumentation

Calibration tests on the chloride analyzer were performed. A low range calibration curve was obtained using standard chloride solutions of 100 ppb and 167 ppb after setting the instrument a full range using a 200 ppb standard solution. Instrumentation drifts were excessive even during relatively short periods of time. Attempts to minimize this drift were unsuccessful. The mechanical components of the analyzer appear to be operating adequately, however further work is necessary to correct deficiencies in the electrical components of the analyzer.

A conductivity indicator-recorder was installed and put into operation at the condenser building sample station. This unit allows the continuous measurement and recording of conductivity of any one of seven streams available at this sample station. A similar unit was installed at the containment building sample station, and will be used to measure conductivity of condensed steam samples when steam is flowing through the reactor.

A 2-hour training class was conducted for Operations personnel on the subject of sampling at the condenser building sample station. The classes included procedures for obtaining liter water samples, for operating the boiler feedwater dissolved oxygen analyzer, and for obtaining off-gas samples.

### 9.2 Oxygen and Hydrogen Gas Analyzer

An in-line analyzer for automatic determination of dissolved gas concentrations in condensed steam samples is being built for the EVELR reactor. The basic equipment design is similar to that currently being used on a corrosion test facility.

The analyzer consists of four basic modules:

- a. Sample programmer,
- b. Gas stripper,
- c. Gas chromatograph, and
- d. Readout system.

During a typical sample cycle, the gases dissolved in the condensed steam are stripped out of solution by means of an inert carrier gas in a closed-loop stripper system. An aliquot portion of the equilibrated gas phase is automatically injected into a gas chromatograph. The hydrogen and oxygen are separated into two distinct peak forms in the gas chromatograph columns. The readout system integrates the area under each peak and converts the results to a final direct ppm relationship between dissolved gas and analog recorder signal height.

## 10.0 SUB-TASK D-1: FUEL TESTS, ENGINEERING PHYSICS

### 10.1 Summary

The zero power EVESR physics critical test program has been completed, except that the following two tests were omitted for the reasons noted:

- No. 4.1.1.7 Type 304 Stainless Steel Channel versus Zircaloy-2 Channel Worth: Omitted inasmuch as it appears that Type 304 stainless steel channels will not be necessary to attain a maximum  $k_{eff}$  (shutdown)  $\leq 0.99$  with any 11 main control rods fully inserted.
- No. 4.1.1.10 Relative Worth of Alternate Fuel Bundles: Omitted inasmuch as no gross unexplained discrepancies on a bundle versus bundle basis were observed.

The low power tests will be started during the latter part of February 1964. Results of the latter tests will be reported in the next quarterly report.

Additional tests requiring the use of a modified spare fuel bundle which allowed selective unloading of the bundle were performed in the flooded and unflooded minimum and full core loadings. The pulse neutron source was made operable in time to measure the central fuel bundle worth (cold, flooded, all rods in full core), the shutdown margin with a maximum worth control rod withdrawn from the cold, flooded full core, as well as shutdown margin as a function of control rod insertion for the normal and inverse patterns. The latter measurements were made for steps from "just subcritical" to all 12 main rods fully inserted.

Table 10-1 and Figure 10-1 summarize the results of these tests, illustrating the comparison between calculated and measured results. The principal differences noted between the predicted and measured results lie in two areas - namely, minimum critical loadings and control rod strengths. These differences are now understood. The significance of these differences affects three general areas of reactor operation i.e., (a) excess reactivity at operating conditions, (b) sufficient control strength to assure adequate shutdown margin, and (c) effects on the hazards evaluation of accidents involving control rods. These matters are discussed in the body of this report.

### 10.2 Description of Critical Measurements

#### 10.2.1 Minimum Criticals

##### 10.2.1.1 Approach to Critical Unflooded

The EVESR minimum critical unflooded core was predicted to be 12 ± 1 bundles. The actual loading was 17 bundles with fuel loaded as illustrated by Figure 10-2. This 17-bundle core had a  $k_{eff} = 1.0027 \pm 0.0003$  at 52°F with all rods out. (This is equivalent to 1.0048 at 68°F.)

TABLE 10-1

EVESR CRITICAL RESULTS VERSUS PREDICTIONS

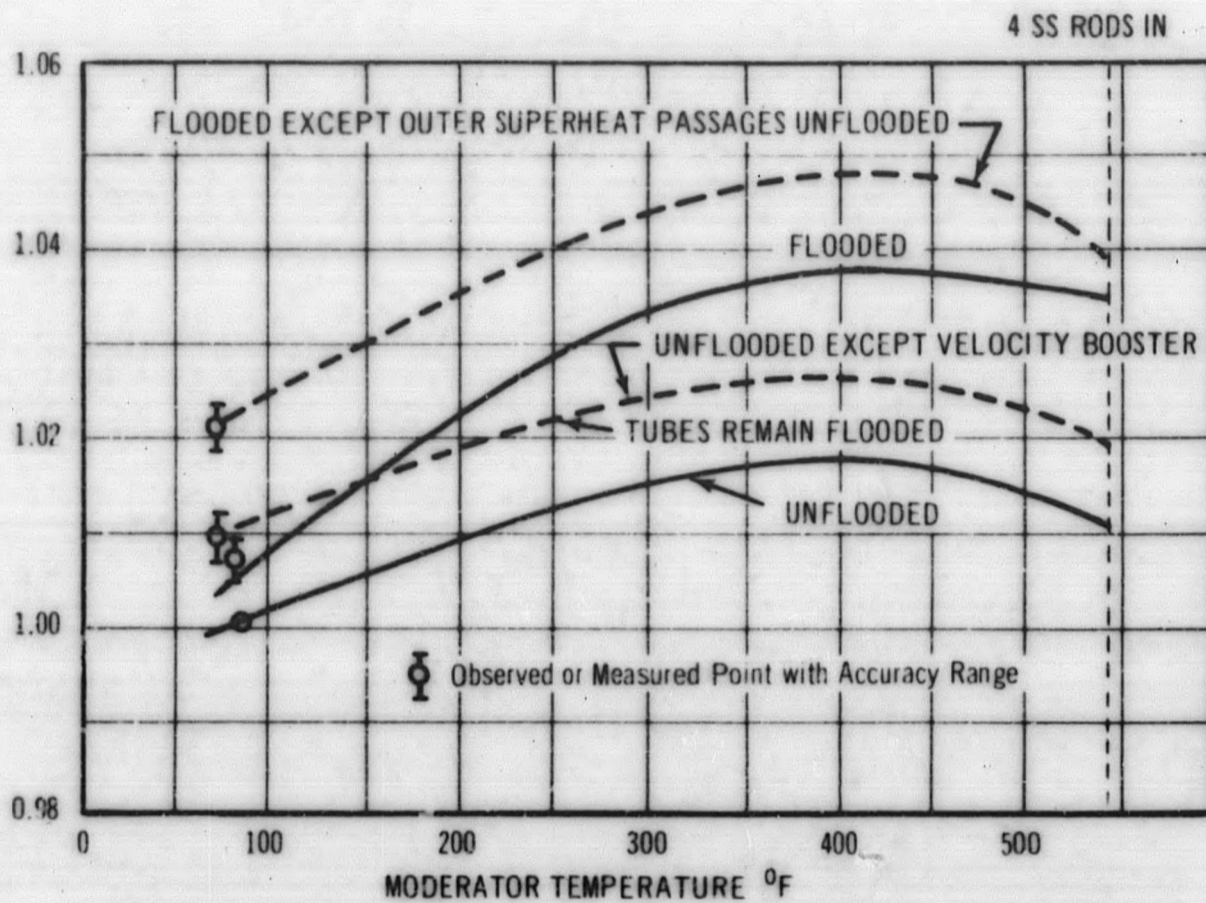
<u>Core Measurements with All Rods Out</u>	<u>Predicted</u>	<u>Measured</u>
Unflooded Minimum Critical Size at 52 F	12 ±1 Bundles	17 Bundles
Flooded Minimum Critical Size at 62 F	11 ±1 Bundles	14 Bundles
Unflooded Temperature Coefficient, 52 to 147 F	0.015% Δk/°F	0.011% Δk/°F
<u>Full Core Measurements</u>		
Control Worth Unflooded:		
Worth of Four Auxiliary Scram Rods, Cold	1.0% Δk	0.75% Δk
Worth of Four Auxiliary Scram Rods, Hot	1.4% ±0.4% Δk	0.86 ±0.08% Δk
Control Worth Flooded (Room Temp Unless Noted)		
*Worth of Inner Bank of Four Rods (Eight Outer Rods In)	8.7 ±1.3% Δk	9.3 ±1.0% Δk
Worth of Outer Bank of Eight Rods (Four Inner Rods In)	10.5 ±1.6% Δk	6.5 ±0.5% Δk
*Worth of 12 Regular Control Rods	15.0 ±2.3% Δk	12.4 ±1.0% Δk
Worth of Four Auxiliary Scram Rods	0.7 ±0.1% Δk	0.6% Δk
Worth of Four Auxiliary Scram Rods, Hot	1.1 ±0.3% Δk	0.57 ±0.05% Δk
Worth of One Inner Rod (11 Rods In)	1.5 ±0.2% Δk**	3.1 ±0.3% Δk
<u>Temperature Effects</u>		
Temperature Coefficient, Unflooded, Full Core		
60 to 180 °F	+0.0111% Δk/°F	+0.0101 ±0.0019 Δk/°F
~510 °F	-0.013 ±0.003	-0.009
Temperature Coefficient, Flooded, Full Core		
81 to 168 °F	+0.010 ±0.003	+0.0123 ±0.0005
~510 °F	-0.008 ±0.003	-0.006
Reactivity Effect of Heating from 68 to 545 °F, Flooded, Rods Out	+0.042 ±0.01	+0.030 ±0.01 (Approximate)
Reactivity Effect of Heating from 68 °F to _____		
Peak Core Reactivity, Flooded:		
Stainless Steel Rods In, Outer Rods 63 Percent Withdrawn	-----	+2.9% Δk ±0.2
Stainless Steel Rods In, Outer Rods 100 Percent Withdrawn	+3.6% Δk ±2.0	-----
All Rods In	+1.6% Δk ±2.0	-----

\*Extrapolated from prestartup calculations corrected by limited measurements.

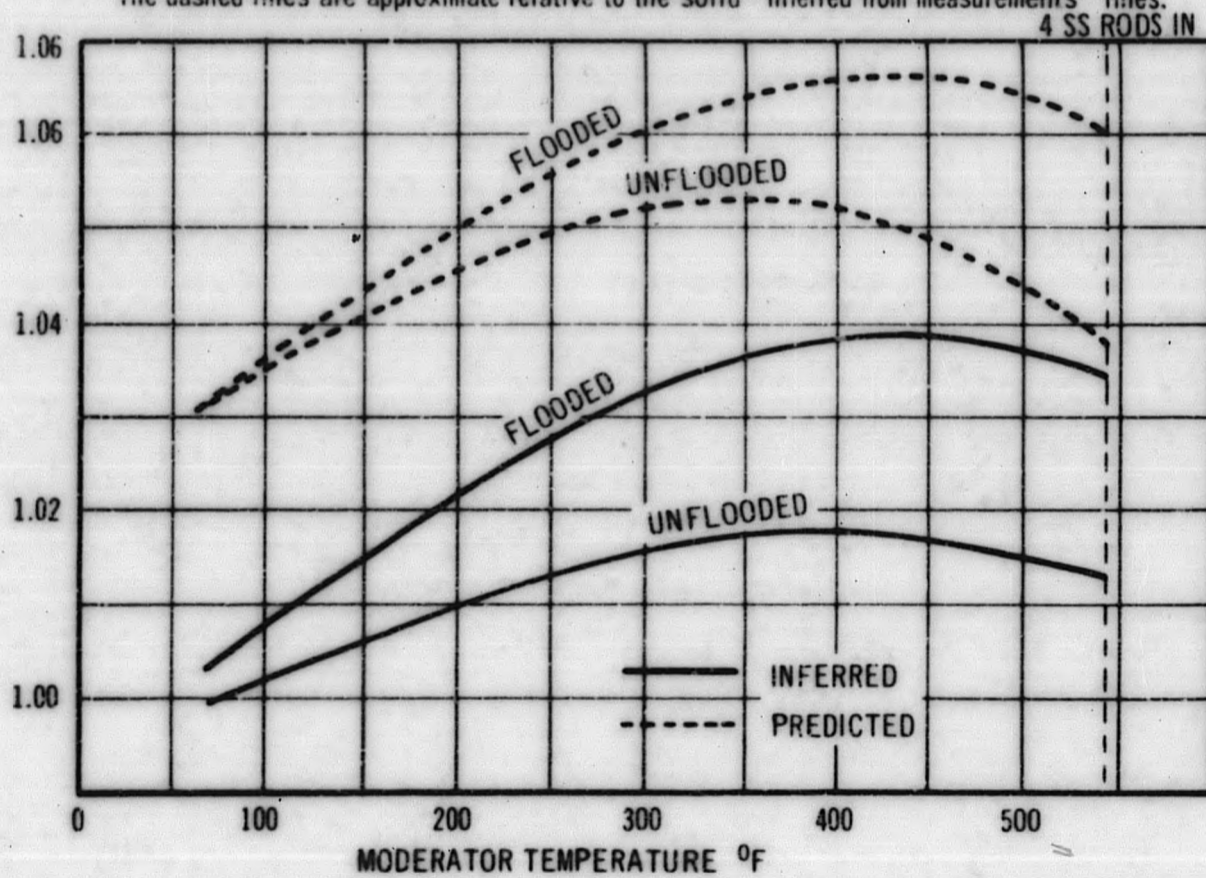
\*\*Not calculated, but extrapolated from another core condition.

TABLE 10-1 (Continued)

<u>Full Core Excess Reactivity</u>	<u>Predicted</u>	<u>Measured</u>
Cold (68°F)		Inferred:
Flooded	0.074 ±0.02	0.071 ±0.01
Unflooded	0.080 ±0.02	0.076 ±0.01
Hot (545°F)		
Flooded	0.116 ±0.02	0.110 ±0.01
Unflooded	0.095 ±0.02	0.088 ±0.01
Unflooded, 1250 F Fuel Temperature, 10 Percent Moderator Voids	0.095 ±0.02	0.078 ±0.01
<u>Unflooding-Flooding Reactivity Effects</u>		
Cold Unflooding Effects:		
Complete	-1.1 ±0.6% Δk/k	-0.8 ±0.4% Δk/k
Outer Steam Pass Only	+1.8 ±0.3	+1.7 ±0.2
Except Velocity Booster Tubes	+0.6 ±0.4	+0.6 ±0.3
Unflooding at 300°F	-1.8 ±0.7	-2.0 ±0.2
Flooding at 545°F	+2.8 ±0.4	+2.2 ±0.2
<u>Minimum Shutdown Margin with Any One Control</u>		
<u>Rod Fully Withdrawn</u>		
350 to 400°F, Flooded	3 ±2% Δk	1.4 ±0.3% Δk
<u>Maximum Fuel Bundle Worth</u>		
68°F Flooded, All Rods In, Zone 1	3.7% Δk	1.6% Δk



\* These curves are inferred from observed control rod calibration curves, using calculations for small portions of the curve which could not be inferred.  
 The dashed lines are approximate relative to the solid "inferred from measurements" lines.



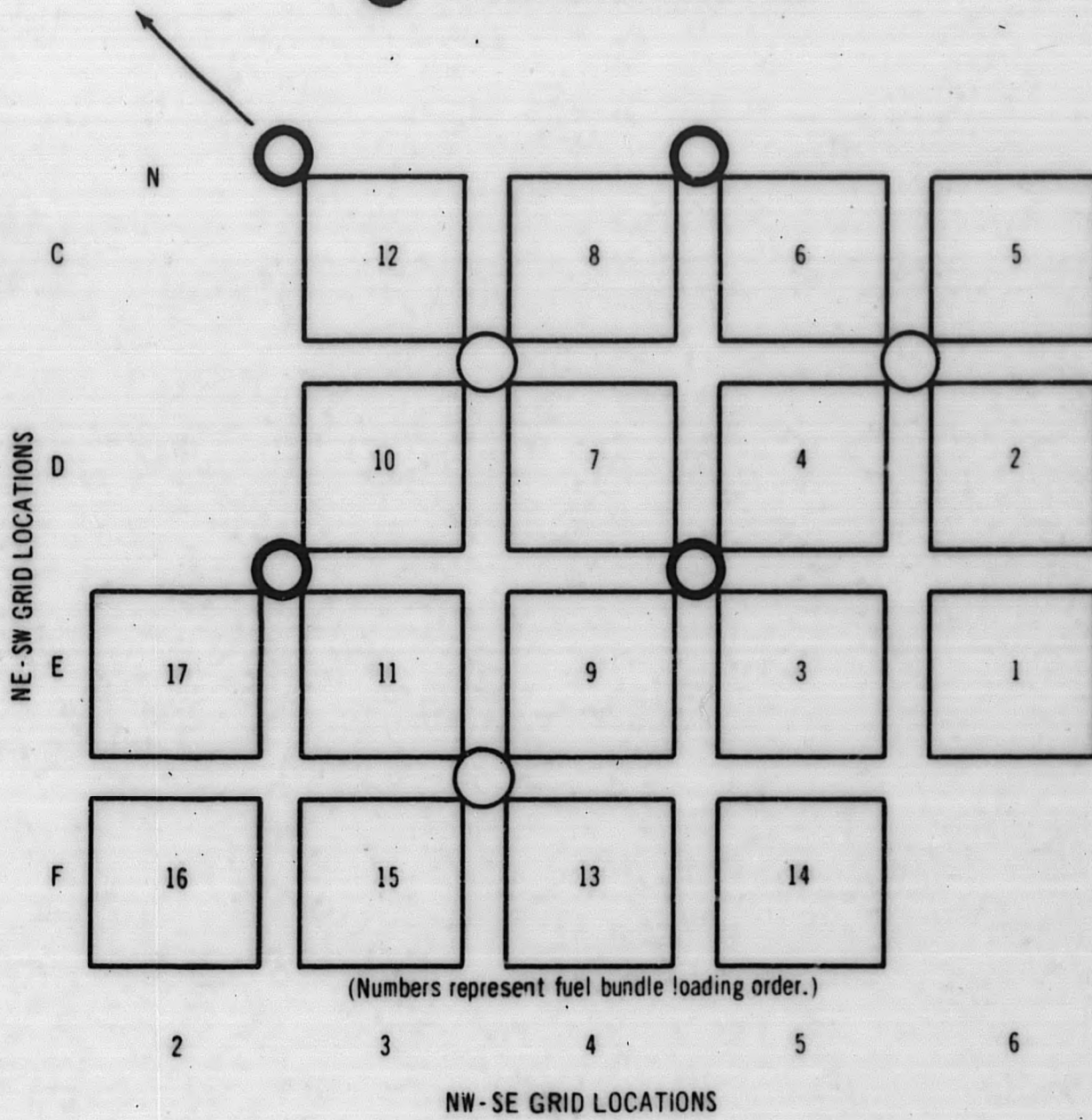
1726-9

Figure 10-1. EVESR, Mk II Core, Multiplication Versus Moderator Temperature

$k_{eff}$  1.0027 ± 0.0003  
 WATER TEMPERATURE 52°F

○ IN-CORE MONITOR GUIDE TUBE

⊙ NEUTRON SOURCE HOLDER TUBE



1726-8

Figure 10-2. EVESR Minimum Unflooded Critical, November 26, 1963

The larger than anticipated difference between the calculated and the actual minimum critical loading is now considered to be due to two principal factors not included in the prestartup analyses:

- a. in-core monitor guide tubes and neutron source tubes (both Type 304 stainless steel) ...  
About 1.2 percent  $\Delta k$ .
- b. Improved representation of the spatial dependence of the thermal neutron spectrum ...  
About 1.5 percent  $\Delta k$ .

For reasons now unknown, the in-core monitor guide tubes and the neutron source holder tubes were omitted from the calculational model schematic illustrated by Figure 4.3 of reference (2). Using the cross-sectional data of reference (2) and the identical calculational model of reference (2), except to include the tubes in the 17-bundle core as loaded, the following results were obtained:

$k_{\text{eff}}$ (17-bundle, unflooded core, 68° F, rods out, variable enrichment, with shims and tubes) .....	1.038
Coarse versus fine mesh correction factor	<u>× 0.9867</u>
	1.024
"As-built" reactivity correction	- 0.010
Calculational versus measured correction	<u>+ 0.007</u>
$k_{\text{eff}}$ (17-bundle, corrected calculation)	1.021
$k_{\text{eff}}$ (17-bundle, measured)	<u>1.005</u>
Difference	0.016

The 1.6 percent reactivity overprediction is within the  $\pm 2$  percent estimated accuracy of the calculational model. But, all, or at least most, of this overprediction can be explained by the spatial dependence of the thermal neutron spectrum - which is of considerable significance in this particular lattice. For example, if the THERMOS<sup>(3)</sup> code is employed to calculate the thermal utilization rather than the two-region empirical softening correction, and both methods are normalized to agree with the 3.4 percent enriched EVESR preliminary critical arrays of more than a year ago, the calculated  $k_{\text{eff}}$  for the present core with its 5.3 percent average enrichment would be reduced by about 1.5 percent. Although the THERMOS model is theoretically better founded, it appeared in the past to overestimate the relative captures in water. However, it has been reported that recent improved measurements of thermal utilization are leading to good agreement between THERMOS and experiment.

Other factors (considered to be small) which may contribute to a loss in reactivity of the minimum critical loading include:

- a. Instrumentation: The minimum critical included the quarter core containing flux wire tubes and thermocouples.
- b. Edge effects: The treatment of edge effects in the minimum critical is more important than the full core. It may be that inadequate representation of the spatial effects near the core-reflector interface has contributed to a calculational error in the minimum loading that will be of less importance in the full core.

10.2.1.2 Approach to Critical Flooded

The EVESR minimum critical flooded core was predicted to be 11 ±1 bundles. The actual loading was 14 bundles with fuel loaded in the same order as illustrated by Figure 10-2 for the unflooded minimum critical. This 14-bundle core had a  $k_{eff} = 1.0027 \pm 0.0002$  at 62°F.

The factors discussed in explaining the discrepancy between the predicted versus measured minimum unflooded critical also apply in the case of the flooded minimum critical. Post-measurement analyses gave the following uncorrected value of  $k_{eff}$  for a 14-bundle core loading:

$k_{eff}$  (14-bundle, flooded, 68°F, rods out, variable enrichment, omitting shims and monitor and source tubes) . . . . . 1.0600

Applying the corrections of reference (2),

Coarse versus fine mesh correction factor . . . . .	~ 0.99
	<u>1.049</u>
As built reactivity correction . . . . .	- 0.008
Calculational versus measured correction* . . . . .	- 0.004
Discrete correction . . . . .	- 0.012
In-core monitor and neutron source tubes. . . . .	- 0.011
Thermal neutron spatial dependence correction* . . . . .	- <u>0.015</u>
$k_{eff}$ , corrected	0.999

a corrected value of  $k_{eff}$  of approximately "just critical" was obtained.

It is thus apparent that incorporating the two factors discussed in paragraph 10.2.1.1 preceding brings the flooded minimum critical prediction into agreement with the actual measurement.

10.2.2 Loading to Excess Reactivity

10.2.2.1 Unflooded

The "just critical" control rod patterns for the unflooded full core loading at 49°F are shown in the following tabulation. The auxiliary scram control rods are fully withdrawn in each case.

\*It has been noted that the use of THERMOS would have made it possible to combine these two corrections into a single +0.011  $\Delta k$  for both the unflooded and flooded core calculations.



<u>Withdrawal Pattern*</u>	<u>Outer Main Rods Position</u>	<u>Inner Main Rods Position</u>
Normal	100 Percent Withdrawn	10 Percent Withdrawn
Banked	27 Percent Withdrawn	27 Percent Withdrawn
Inverse	Fully Inserted	56 Percent Withdrawn

Comparing the observed just critical control rod patterns to the predicted patterns - Figure 4.6, reference (2) - it is apparent that the calculations have underpredicted the worth of the inner main control rods and overestimated the worth of the outer main control rods. The reason for this discrepancy is explained in paragraph 10.2.3.

10.2.2.2 Flooded

The just critical control rod patterns for the flooded full core loading at 75°F are shown in the following tabulation. Auxiliary scram control rods are fully withdrawn in each case.

<u>Withdrawal Pattern*</u>	<u>Outer Main Rods Position</u>	<u>Inner Main Rods Position</u>
Normal	63 Percent Withdrawn	Fully Inserted
Banked	22.1 Percent Withdrawn	22.1 Percent Withdrawn
Inverse	Fully Inserted	38.7 Percent Withdrawn

As for the unflooded full core, a comparison of the observed versus the predicted just critical control rod patterns [Figure 4.8, reference (2)] makes it apparent that the calculations have underpredicted the worth of the Type 304 stainless steel inner control rods and overestimated the worth of the Type 304 stainless steel with boron outer main control rods.

10.2.3 Control Rod Worth

Table 10-2 illustrates the predicted versus measured (or inferred) control rod worths for two extreme core conditions: i.e., cold, flooded and hot, unflooded with 10 percent voids (operating condition). A number of these measurements are extrapolated from limited measurements using the shape of the rod worth curves of reference (2). However, numerous cross checks were used to provide good confidence that their accuracies lie within the stated limits.

\*See \*footnotes pp 31-32, reference (2).

TABLE 10-2

EVESR MAIN CONTROL SYSTEM WORTH - PERCENT  $\Delta k$   
MEASURED VERSUS CALCULATED ( OR PREDICTED)

<u>Description*</u>	<u>EVESR FHSR APED-3958 10-1-62</u>	<u>EVESR Pre-Startup Report, GEAP-4213, 4-12-63</u>	<u>"Inferred" from Startup Measure- ments (12-63/2-64)</u>	<u>Current (2-21-64) Analytic Model</u>
<u>68°F Flooded:</u>				
Inner Rods:				
Alone	4.7	4.6	6 ±1	6.7
Shadowed	7.6	8.3	9.3 ±1	9.4
Single Rod (all rods in)	1.5	---	3.1 (PNS)**	3.2
Outer Rods:				
Alone	5.4	6.3	4.0 ±0.5	3.8
Shadowed	8.3	9.7 ±0.6	6.5 ±0.5 (PNS)**	6.4
Single Rod (all rods in)	1.3	---	< 1.3	---
Inner and Outer Rods	13.0	15.4	12.4 ±0.8	13.1
<u>545°F Unflooded, 10 Percent Voids:</u>				
Inner Rods:				
Alone	6.6	6.3	7.5 ±1	8.4
Shadowed	9.6	---	11.5 ±1	12.6
One of Four (outer rods out)	1.6	---	2.1	2.1
One rod (11 rods out)	---	---	---	2.2
Maximum rod	2.7	---	3.7	---
Outer Rods:				
Alone	9.9	---	6.5 ±1	7.6
Shadowed	12.9	14.5	10 ±1	10.8
Maximum rod	3.3	---	< 3	---
Inner and Outer Rods	19.5	20.8	17.5 ±1.5	19.2

\*The four auxiliary scram rods are completely withdrawn.

\*\*Pulsed neutron source measurement.

The most significant differences noted in comparing predictions to measurements of actual rod worths is the consistent under-prediction of the four Type 304 stainless steel inner control rod worths and the over-prediction of the worth of the eight Type 304 stainless steel with Boron outer main control rods. It is, however, encouraging to note that our current analytic model (Table 10-2) calculates control worths which are in excellent agreement with the measurements. Two changes were made to our original model to provide this agreement:

- a. As noted by reference (2), and based on preliminary results of the EVESR preliminary critical reported by Table II, C.16 of reference (1), it was suspected that the worth of the Type 304 stainless steel control rods was being overpredicted by about 20 percent. Accordingly, to assure adequate shutdown margin, the calculated values for the Type 304 stainless steel control rods were decreased by multiplying by 0.828. Subsequent analyses of the EVESR preliminary critical measurements indicated [Table 3-1, reference (4)] that the calculational model for determining Type 304 stainless steel control rod required no correction. Hence, in the current calculational model of EVESR Type 304 stainless steel control rod strength the 0.828 multiplicative correction factor was omitted. Of lesser significance, the 0.965 multiplicative correction factor for the eight outer control rods was also omitted.
- b. The old model (three-group diffusion theory) omitted the following details in the EVESR core:

- Power flattening shims (Inconel)
- In-core monitor guide tubes (Type 304 stainless steel)
- Neutron source holder tubes (Type 304 stainless steel)
- Auxiliary scram rod sheaths (Type 304 stainless steel)
- Variable enrichment
- Peripheral shroud (Type 304 stainless steel)
- Coarse mesh

The new model (also three-group diffusion theory) uses a finer grid mesh (54 by 54 point quarter core) and incorporates the above material details. Due to the fact that these relatively strongly absorbing materials are concentrated toward the outer control rod region, it is now apparent that these materials have reduced the worth of the outer rods and may have enhanced the worth of the inner control rods.

Auxiliary scram rod worth values - predicted versus measured - are compared in Table 10-1. As with the outer main control rods, the worth of the auxiliary scram rods was over-predicted. It is expected that the inclusion of the details of the current calculational model would provide good agreement with measurements. However, inasmuch as the measurements show that the scram rods meet technical specification requirements (the worth of the four rods must exceed 0.5 percent  $\Delta k/k$  in the "normal" control rod pattern, with the reactor critical) it is not planned to carry out these expensive calculational verifications.

#### 10.2.4 Temperature Coefficients

Table 10-3 illustrates the measured versus predicted temperature coefficient for the unflooded minimum critical and the unflooded and flooded full cores. In addition to this table, the temperature coefficient may be obtained graphically from Figure 10-1. The agreement between predicted and measured temperature coefficients is seen to be very good. There is an indication, however, from the predicted versus "inferred" from startup measurements curves that the temperature coefficient is slightly more positive than predicted.

#### 10.2.5 Full Core Excess Reactivity

Table 10-4 illustrates the predicted versus inferred full core excess reactivity.

In examining this table of full core excess reactivity, three items of significance for discussion are suggested:

- a. How accurate are the inferred numbers, and how were they obtained?
- b. All of the inferred numbers fall within the expected accuracy of the predictions. Hence this core is expected to provide burnup as per design specifications.
- c. If (b) is true, why was the reactivity of the minimum criticals overpredicted by about 3 percent  $\Delta k$ ?

In answering (a), the full core excess reactivity is largely due to the strength of four Type 304 stainless steel inner control rods. Table 10-4 indicates that our current model for calculating the strength of the EVESR main control rods is excellent. The inferred numbers were obtained by slightly diminishing results from this calculational model. Where the eight outer rods were also partially inserted their strengths were obtained directly from calibration curves of these rods with the inner rods inserted. It is expected that the inferred numbers in Table 10-4 are accurate to within  $\pm 0.01 \Delta k$ .

In discussing (b), it is necessary to answer (c). From the curve of  $k_{eff}$  versus water temperature (Figure 10-1), it is apparent that the overall temperature effect between 68°F and 545°F is as predicted. It also appears that the cold full core excess reactivity was accurately predicted, while the cold minimum criticals were missed by about a 3 percent  $\Delta k$  overprediction. The latter has been explained (10.2.1): the "accurate" prediction of the cold full core excess reactivity is partially due to compensating errors,

Calculational Corrections, Unflooded  
Refer to TABLE A.15, Addendum to Reference (2)

	<u>8-20-63</u>	<u>1-29-64</u>
Spatial Thermal Neutron Spectrum (THERMOS)	0.0	-1.5
Inconel Shims	-1.7	-0.7
In-Core Monitor Guide and Neutron Source Tubes	-0.5	-1.0
NET	-2.2% $\Delta k$	-3.2% $\Delta k$

TABLE 10-3  
TEMPERATURE COEFFICIENT - MEASURED VERSUS PREDICTED  
PERCENT  $\Delta k/k$  PER °F

<u>Predicted</u>		<u>Core Description</u>	<u>Measured</u>	
<u>Temp Range</u>	<u>Coefficient</u>		<u>Temp Range</u>	<u>Coefficient</u>
		<u>Unflooded, Minimum Critical</u>		
68 to 212 F	+ 0.0102	17-Bundle 11-Bundle	52 to 147 F	+ 0.011 ±0.001
		<u>Unflooded, Full Core</u>		
68 to 212 F	+ 0.0111	Stainless steel rods in; outer rods 100 percent withdrawn at 60 F to 60 percent withdrawn at 180 F	60 to 180 F	+ 0.0101 ±0.001
~510°F	-0.011	Stainless steel rods in; outer rods 100 percent withdrawn ----- Stainless steel rods in; outer rods 50 percent withdrawn	~510°F	-0.009
	-0.016	Stainless steel rods in; outer rods out ----- All rods in		
		<u>Flooded, Full Core</u>		
68 to 212°F	+ 0.0127	Stainless steel rods in; outer rods 60 percent withdrawn at 81 F to 45 percent withdrawn at 168 F	81 to 168°F	+ 0.0123 ±0.0005
68 to 212°F	+ 0.0071	Stainless steel rods in; outer rods out ----- All rods in		
~510°F	-0.005	Stainless steel rods in; outer rods 38 percent withdrawn	~510°F	-0.006
~510°F	-0.011	Stainless steel rods in ----- All rods in		

TABLE 10-4  
FULL CORE EXCESS REACTIVITY ( $\Delta k$ )  
EVESR Mk II CORE AT STARTUP

<u>Core Condition</u>	<u>Predicted</u>	<u>"Inferred"</u>
Cold (68°F):		
Flooded	0.074 ±0.02	0.071 ±0.01
Unflooded	0.080 ±0.02	0.076 ±0.01
Hot (545°F):		
Flooded	0.116 ±0.02	0.110 ±0.01
Unflooded	0.095 ±0.02	0.088 ±0.01
Unflooded, 1250°F Fuel Temperature, 10 Percent Moderator Voids	0.085 ±0.02	0.078 ±0.01

The above difference is 1 percent  $\Delta k$  while the cold unflooded difference noted in Table 10-4 is 0.4 percent ±1 percent  $\Delta k$ . These numbers are similar, although there is some indication that approximately 0.6 percent  $\Delta k$  is gained in going from a minimum critical to a full core loading - as compared to the January 29, 1964 calculational model. As discussed in the preceding paragraph the inferred cold unflooded full core excess reactivity was obtained from the control rod worth calculational model - and its accuracy is ±1 percent  $\Delta k$ .

The following table illustrates the expected normal rod pattern at startup during operation at rated power:

$k_{eff}$ , unflooded, 1250°F fuel, 10 percent voids in moderator	1.078 ±0.01
Equilibrium Xe, Sm	-0.02
	1.058 ±0.01

		<u>Outer Rods</u>	<u>Inner Rods</u>
Rod pattern, no Xe, Sm, Mk II startup core*	Minimum $k_{eff}$ , maximum rods:	Out	25 Percent Withdrawn
	Nominal:	Out	10 Percent Withdrawn
	Maximum $k_{eff}$ , minimum rods:	20 Percent Withdrawn	Full In
Rod pattern with Xe, Sm, Mk II startup core*	Minimum $k_{eff}$ , maximum rods:	Out	45 Percent Withdrawn
	Nominal:	Out	30 Percent Withdrawn
	Maximum $k_{eff}$ , minimum rods:	Out	10 Percent Withdrawn

\*12.5 MWt; inner rod strength 0.081 ±0.01

10.2.6 Unflooding-Flooding Reactivity Effects

Table 10-5 summarizes predicted versus measured full core unflooding effects at room temperature and 300°F. Flooding effects at 545°F are also shown.

The measurements reported in Table 10-5 are seen to be in good agreement with predictions, except that unflooding effects are generally a little less positive (or more negative) than predicted. This is especially true in the cold condition. The measured core condition more nearly approximates the "Four Stainless Steel Rods In" condition as the outer rods withdrawn 63 percent leaves only 11 percent of their worth inserted. Refer to Figure 10-1 for inferred estimates of unflooding-flooding reactivity effects not tabulated in Table 10-5.

TABLE 10-5  
UNFLOODING-FLOODING REACTIVITY EFFECTS  
PERCENT  $\Delta k/k$

<u>Parameter</u>	<u>Predicted*</u>			<u>Measured</u>
	<u>All Rods Out</u>	<u>Four Stainless Steel Rods In</u>	<u>All Rods In</u>	
Unflooding, Cold:				
Complete	+0.5(+0.7)	-0.5%(0)	-1.7(-1.1)	-0.8 ±0.4
Outer Steam Pass*	+2.7	+2.1	+1.5	+1.7 ±0.2
Velocity Booster	+1.4	+1.0	+0.1	+0.6 ±0.3
				Stainless Steel Rods In, Outer Rods 63 Percent Withdrawn
Flooded**				
Unflooding at 300°F	-0.4(-0.3)	-1.1(-0.8)	-2.5(-1.9)	-2.0 ±0.2 at 340°F Stainless Steel Rods In, Outer Rods: 50 Percent Withdrawn (Unflooded); 34 Percent Withdrawn (Flooded)
Flooding at 545°F	+2.2(1.8)	+2.4(+2.3)	+3.2(+3.4)	+2.2 ±0.2 at 520°F Stainless Steel Rods In, Outer Rods: 54 Percent Withdrawn (Unflooded); 35 Percent Withdrawn (Flooded)

\*Predicted by reference (2): Values shown in parenthesis were predicted by reference (1).

\*\*These values were not predicted by either reference (2) or (1), inasmuch as their existence and magnitude were not recognized until September 1963. These values were calculated and reported, prior to their measurement, for inclusion in the Sixth Quarterly Progress Report on November 27, 1963.

Details of the measurements, predictions, and evaluations are included in the following sub-paragraphs.

#### 10.2.6.1 Special Bundle Flooding-Unflooding Tests, Unflooded Core

One of the spare fuel bundles (SP2L designation) was modified to permit the bundle to be flooded, its outer steam passage (OSP) to be unflooded in steps, and, by means of air flow through the bundle, to permit the unflooding of both the inner and outer steam passages leaving only the velocity booster tubes (VB) flooded. The complete unflooding of the special bundle required that it be attached to a strongback and inverted to drain. Since this was a very time-consuming operation, it was not done for every position. If this was not done, however, the condition (unflooded, partially flooded, or completely flooded) of the velocity boosters was not known for completely unflooded bundle tests. It also should be noted that small holes in the bottom regions of the velocity boosters permitted some water to seep out of the tubes during the progress of the measurement. Also, subsequent inverting and draining showed that, in some cases, some water from the superheat passages remained in the bottom portion of the process tubes. As a result of these uncertainties, the data presented below for the test condition of "complete unflooding except VB's" are designated "VB?" to indicate that the presence or absence of water in the steam passages and velocity boosters was either not precisely known or did not correspond to the desired condition. The large uncertainties in the D-1 position (Zone 4) measurements are due to the method of rod positioning used to measure the flooding effects.

##### 10.2.6.1.1 Unflooded Minimum Critical (Cold)

The below table illustrates the predicted (a) versus measured (b) reactivity changes which occurred as a result of unflooding (partial and complete) the modified spare fuel bundle while in core position D 5 (Zone 3) of the 17-bundle minimum unflooded cold critical core:

<u>Effect</u>		<u>Reactivity Change, Percent <math>\Delta k/k</math></u>
Complete unflooding	(a)	-0.05 $\pm$ 0.05 - predicted
the spare only	(b)	-0.04 $\pm$ 0.01 - measured
Unflooding OSP only of	(a)	+0.27 $\pm$ 0.07
the spare bundle	(b)	+0.15 $\pm$ 0.02
Unflooding except VB's	(a)	+0.12 $\pm$ 0.05
remain flooded	(b)	-0.02 $\pm$ 0.01 (VB?)

##### 10.2.6.1.2 Unflooded Full Core Loading (Cold)

The below table illustrates the results of predicted (a) versus measured (b) special bundle flooding-unflooding tests in the cold, unflooded full core loading:



Effect	Reactivity Change, Percent $\Delta k/k$					
	Zone 1	Zone 2	Zone 3	Zone 4	Zone 5	32 Bundles
Complete unflooding (a)	+0.023	-0.016	-0.030	-0.018	-0.01	+0.4
	+0.02	-0.02	+0.02	+0.02	+0.02	
the spare only (b)	+0.015	+0.014	+0.004	+0.005	+0.005*	+0.2
Unflooding OSP only (a)	+0.13	+0.09	+0.12	+0.04	+0.03	+2.4
	+0.03	+0.02	+0.03	+0.02	+0.02	
of the spare bundle (b)	+0.131	+0.077	+0.099	+0.044	+0.04*	+2.3
				+0.015		
Unflooding except (a)	+0.06	+0.04	+0.06	+0.01	0	+1.0
	+0.02	-0.02	+0.02	+0.01	+0.02	+1.0
VB's remain flooded (b)	+0.103	+0.042	+0.072	+0.019	+0.01*	+1.4
				-0.008		

\*Not Measured

Inasmuch as it was shown by earlier calculations that the above unflooding effects are dependent on the bundle enrichment and clad type, and since the spare bundle differs in both of these respects from most of the bundles whose positions it occupied for these measurements, it was thought that a better interpretation of the measured results would be obtained by applying the following expression:

$$\Delta k (\text{unflooding effect}) = \sum_{i=1}^{32} \left[ \Delta k_m^{SB} + (\Delta k_c^{AB} - \Delta k_c^{SB}) \right]_i$$

where the subscript

- i refers to each of 32 bundle locations,
- m refers to a measured result,
- c refers to a calculated (predicted) reactivity change,
- SB refers to the "special bundle", and
- AB refers to the actual bundle.

The above expression may be rewritten in the following forms:

$$\begin{aligned} \Delta k (\text{unflooding effect}) &= \sum_{i=1}^{32} \Delta k_c^{AB} + \sum_{i=1}^{32} (\Delta k_m^{SB} - \Delta k_c^{SB})_i \\ &= \Delta k_c^{\text{full core}} + \sum_{i=1}^{32} (\Delta k_m^{SB} - \Delta k_c^{SB})_i \end{aligned}$$

With this interpretation, the measured full core effects, with the four central Type 304 stainless steel control rods fully inserted, become:

<u>Effect</u>	<u>Predicted</u>	<u>Measured</u>
Cold, unflooding	-0.5% $\Delta k/k$	-0.1% $\Delta k/k$
OSP unflooding, cold	+2.1	+2.0
Cold, unflooding except VB's	+1.0	+1.3 0.3

10.2.6.2 Special Bundle Flooding-Unflooding Tests, Flooded Core

Additional modifications to the bundle made it possible to estimate, more correctly, the condition of the velocity booster tubes for the condition of all unflooded except the velocity booster tubes.

10.2.6.2.1 Flooded 15-Bundle Core

The following table illustrates the predicted (a) versus measured (b) reactivity change which occurred as a result of unflooding (partial and complete) the modified spare fuel bundle while in core position D-5 (Zone 3) of a 15-bundle flooded cold core:

<u>Effect</u>		<u>Reactivity Change, Percent <math>\Delta k/k</math></u>	
Complete unflooding the spare only	(a)	-0.03	$\pm 0.03$ Predicted
	(b)	+0.044	$\pm 0.015$ Measured
Unflooding OSP only of the spare bundle	(a)	+0.27	$\pm 0.03$
	(b)	+0.251	$\pm 0.015$
Unflooding, except VB's remain flooded	(a)	+0.16	$\pm 0.04$
	(b)	+0.13	$\pm 0.015$ (VB?)

10.2.6.2.2 Flooded Full Core Loading (Cold)

The following table illustrates the results of predicted (a) versus measured (b) special bundle flooding-unflooding tests in the cold, flooded full core loading. It should be noted that the predicted values were obtained from core configurations with only four central stainless steel rods in. However, the normal control rod withdrawal sequences included the eight outer main rods withdrawn 60 to 65 percent, as well as the full insertion of the four central stainless steel rods. The actual pattern, as compared to the calculation pattern, is a reduced core size, thereby enhancing the negative leakage effects of unflooding. Hence, unflooding effects would be expected to be a little less positive (or more negative) than calculations indicate.

Effect	Reactivity Change, Percent $\Delta k/k$					
	Zone 1	Zone 2	Zone 3	Zone 4	Zone 5	32 Bundles
Complete unflooding (a)	+0.07	+0.01	+0.03	-0.01	-0.01	+0.4 ±0.8
	±0.03	±0.03	±0.03	±0.02	±0.02	
the spare only (b)	+0.014	-0.008	+0.009	-0.032	-0.023	-0.3
Unflooding OSP only (a)	+0.12	+0.09	+0.11	+0.04	+0.02	+2.2 ±0.6
	±0.03	±0.02	±0.02	±0.02	±0.01	
of the spare bundle (b)	+0.100	+0.061	+0.082	+0.036	+0.011	+1.7
Unflooding, except (a)	+0.10	+0.06	+0.08	+0.02	+0.01	+1.5 ±0.8
	±0.04	±0.03	±0.03	±0.02	±0.01	
VB's remain flooded (b)	+0.066	+0.030	+0.055	+0.013	-0.003	+0.9

Using the interpretive equation of paragraph 10.2.6.1.2, the measured full core effects, with the four central Type 304 stainless steel control rods fully inserted and the eight outer rods inserted 35 to 40 percent, become:

	Predicted		Measured
	Stainless Steel Rods In	All Rods	
Cold, unflooding	-0.5% $\Delta k/k$	-1.7% $\Delta k/k$	-0.8 ±0.4% $\Delta k/k$
OSP unflooding, cold	+2.1	+1.5	+1.7 ±0.2
Cold, unflooding except VB's	+1.0	+0.1	+0.6 ±0.3

10.2.C.2.3 Special Bundle Flooding-Unflooding Tests with Zircaloy-2 Water Displacers

Calculations have shown that reducing the bundle water/fuel ratio in turn reduces the effect of cold unflooding of the outer superheat passes (OSP). Zircaloy water displacers were fabricated to form an "egg-crate" around the process tubes which in effect reduces the water/fuel ratio from a nominal 3.2 to 2.9. The unflooding effects with the Zircaloy water displacers inserted were measured in only one core position (Zone 1) for both the unflooded and flooded full cores. No predictions were made of the effects, other than full core calculations which indicated a reduction in the OSP unflooding effect to about 70 percent of the effect without Zircaloy displacers.

Effect	Reactivity Change, Percent $\Delta k/k$	
	Unflooded, Zone 1	Flooded, Zone 2
Complete unflooding the spare only	Not measured	-0.010
Unflooding OSP only of the spare bundle	+0.085 ±0.01	+0.069
Unflooding, except VB's remain flooded	+0.022 (VB?)	+0.038

The above measurements are in apparent agreement with the overall prediction. A more extensive analysis will be made if safety considerations necessitate some form of correction to reduce OSP unflowing effects.

10.2.6.2.4 Special Bundle Flooding-Unflooding Tests.

A second way to reduce the bundle water/fuel ratio is accomplished by placing four UO<sub>2</sub> rods between the process tubes of a Mk II fuel bundle. The incentive for such a "fix" was discussed in the Sixth Quarterly Progress Report. Unflooding effects with four 0.55-inch UO<sub>2</sub> rods in the special bundle were measured and are as follows. No predictions were made of the effects, other than full core calculations which indicated a reduction in the OSP unflowing effect to about 60 percent of the effect without the UO<sub>2</sub> rods.

Effect	Reactivity Change, Percent $\Delta k/k$	
	Flooded, Zone 1	Flooded, Zone 3
Complete unflowing the spare only	-0.017 $\pm$ 0.003	-0.024 $\pm$ 0.003
Unflooding OSP only of the spare bundle	+0.073 $\pm$ 0.003	+0.058 $\pm$ 0.003
Unflooding, except VB's remain flooded	+0.037 $\pm$ 0.003	+0.025 $\pm$ 0.003

The above measurements are in approximate agreement with the overall prediction. These results are essentially identical to the results obtained by using Zircaloy-2 water displacers (10.2.6.2.3).

10.2.7 Minimum Shutdown Margin

Table 10-6 illustrates the predicted versus measured minimum shutdown margin with one maximum strength (inner) control rod fully withdrawn:

TABLE 10-6  
MINIMUM SHUTDOWN MARGIN WITH ANY ONE CONTROL  
ROD FULLY WITHDRAWN, (PERCENT  $\Delta k$ )

<u>Approximate Core Temperature</u>	<u>Predicted*</u>	<u>Measured</u>
350 to 400 °F, Flooded	4% (1.6%)	1.1% $\pm$ 0.5 (PNS at 375 °F) 1.7% (Rod calibration at 390 °F)

\*See footnote Table 10-5

The measured minimum shutdown is less than predicted due to the measured total control worth being less than predicted. Up to 2 percent more shutdown is available by replacing as many as eight Zircaloy channels with Type 304 stainless steel channels. However, it now appears that the use of Type 304 stainless steel channels is not required.

10.2.8 Fuel Bundle Worth

A central (Zone 1) fuel bundle was calculated to have a worth of 3.7 percent  $\Delta k$  in the cold, flooded, all rods in core. A pulsed neutron measurement indicates a worth of only 1.6 percent  $\Delta k$ . This measured versus predicted worth differs more than expected. Although in a safe direction, an understanding of this difference is being sought.

10.2.9 "Just Critical" Control Rod Patterns

Inasmuch as reactor physicists reading this report may wish to verify some of the inferred data in this report, this section contains a tabulation of most observed critical control rod patterns as a function of moderator temperature:

Moderator Temperature (°F)	Control Rod Positions	
	Inner Rods Fully Inserted Except as Noted	
	Outer Rods Withdrawn as Noted	
	Flooded	Unflooded
53	---	100%, Inner 10%
80	61%	---
100	---	83%
120	52.5%	---
130	---	71%
152	---	65%
160	47.5%	---
182	---	60%
200	41.5%	---
240	37.7%	---
280	35.5%	---
320	34.0%	---
350	---	50%
360	33.5%	50%
400	32.7%	50%
435	---	50%
450	33.0%	---
480	---	51%
495	33.7%	---
515-520	35.0%	---
528	37.5%	---
530-532	---	55 to 56%

Inverse Patterns

515°F, Flooded:	Outer Rods	Fully Inserted
	Inner Rods	30.5 Percent Withdrawn
518°F, Unflooded:	Outer Rods	Fully Inserted
	Inner Rods	42 Percent Withdrawn

12-Rods Banked Patterns

515°F, Flooded:	12 Rods	18.2 Percent Withdrawn
518°F, Unflooded:	12 Rods	22.2 Percent Withdrawn

One Central (Type 304 Stainless Steel) Rod Withdrawn

510°F, Flooded:	Outer Rods Fully Inserted:	
	(1) 3 Inner Rods	24 Percent Withdrawn
	(2) 2 Inner Rods	Fully Inserted, and
	3rd Inner Rod	49.3 Percent Withdrawn

(3rd inner rod is adjacent to fully withdrawn rod.)

#### 11.0 SUB-TASK D-2: FUEL TESTS, TEST ENGINEERING

Construction acceptance tests for the R and D panel were completed in February utilizing basic pressure and electrical signals. Calibration of the instrumentation checked out within  $\pm 1.2$  percent. Minor adjustments to pressure transmitters and recorders were required. The pre-power and low power tests for the R and D panel were written and approved.

Several meetings were held with operating personnel to review plans for taking DARE Code data. Revised instructions were issued in preparation for taking data during prepower and low power tests. Several meetings were also held to determine the format for Chemistry R and D data and the data sheets have been prepared.

A revision of the R and D panel instrumentation has been made so that temperature can be indicated at saturated steam conditions (542°F). This will enable a hot calibration check to be made of the instrumentation every time that the reactor is heated up. The existing range of the temperature recorders is 600 to 1200°F which requires the use of millivolt meters to calibrate the thermocouples at saturated steam conditions.

Several 2-hour orientation sessions were conducted on the R and D instrumentation for all EVESR shift personnel. Four 2-hour sessions on the operation and maintenance of the R and D panels were also given for the instrument technician and engineers. Further training sessions are planned after the as-built drawings and operation and maintenance instruction manuals are distributed.

**12.0 SUB-TASK D-3: TEST SPECIFICATIONS**

Test specifications calling out the test conditions to be maintained and the data to be collected at the EVESR site for the Superheat Fuel Development Program have been issued as follows:

Fuel Temperature and Power Level Requirements	Specification A1 Rev. 0 (draft)
Fuel Clad Coupon Irradiation Program	Specification B-1 Rev. 0 (final)
Coolant Chemistry Specifications	Specification C-1 Rev. 0 (final)

It is expected that these specifications will be revised and additional specifications will be issued as necessary to meet the needs of the nuclear superheat fuel development program.



### 13.0 SUB-TASK D-4: DATA PROCESSING

During the last quarter, substantial headway has been made on the implementation of the DARE Code. The PATSE and CORET programs have been put into production status. DARE 5A -- the option for creating the operating charts -- has been put into production and other stages of the system are progressing as scheduled.

The PATSE program was put into production status shortly after the first of the year, and has been used to obtain information for the startup of the reactor. The documentation of this program is now in progress and approximately 40 percent complete.

The CORET program was put into production a few days following the PATSE Code. It was also used to obtain information relevant to the startup of EVESR. The documentation of the code will commence shortly after the preliminary of PATSE is completed.

The DARE 5A option was put into production late in February, and the initial operating charts have been calculated and plotted from the program. The operating charts in conjunction with the EVESR R and D instrumentation will be used to set and maintain the desired test conditions for the MARK II fuel. These charts are reproduced in Figures 13-1 through 13-5, and show the relationship among the following key fuel and reactor operating parameters:

- a. Fuel clad surface temperature,
- b. Superheated steam exit temperature,
- c. Reactor power level, and
- d. Steam coolant flow.

The constants used in the DARE 5 calculation of the operating curves are shown in Tables 13-1, 13-2, and 13-3. The clad temperatures shown on the curves are the most probable values, and do not include allowance for calculation uncertainties or hot-spot factors.

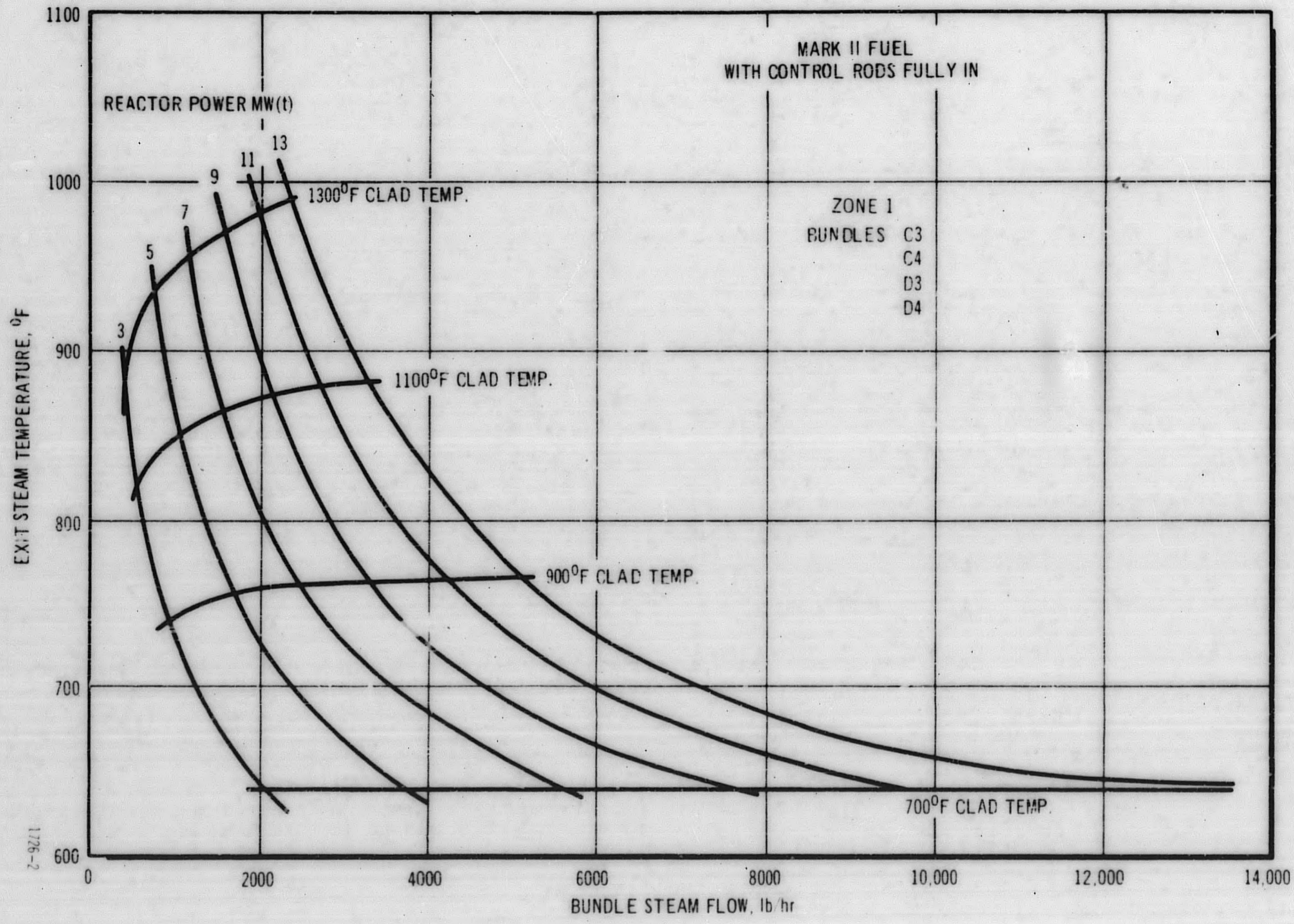


Figure 13-1. EVESR Mark II Fuel Operating Parameters

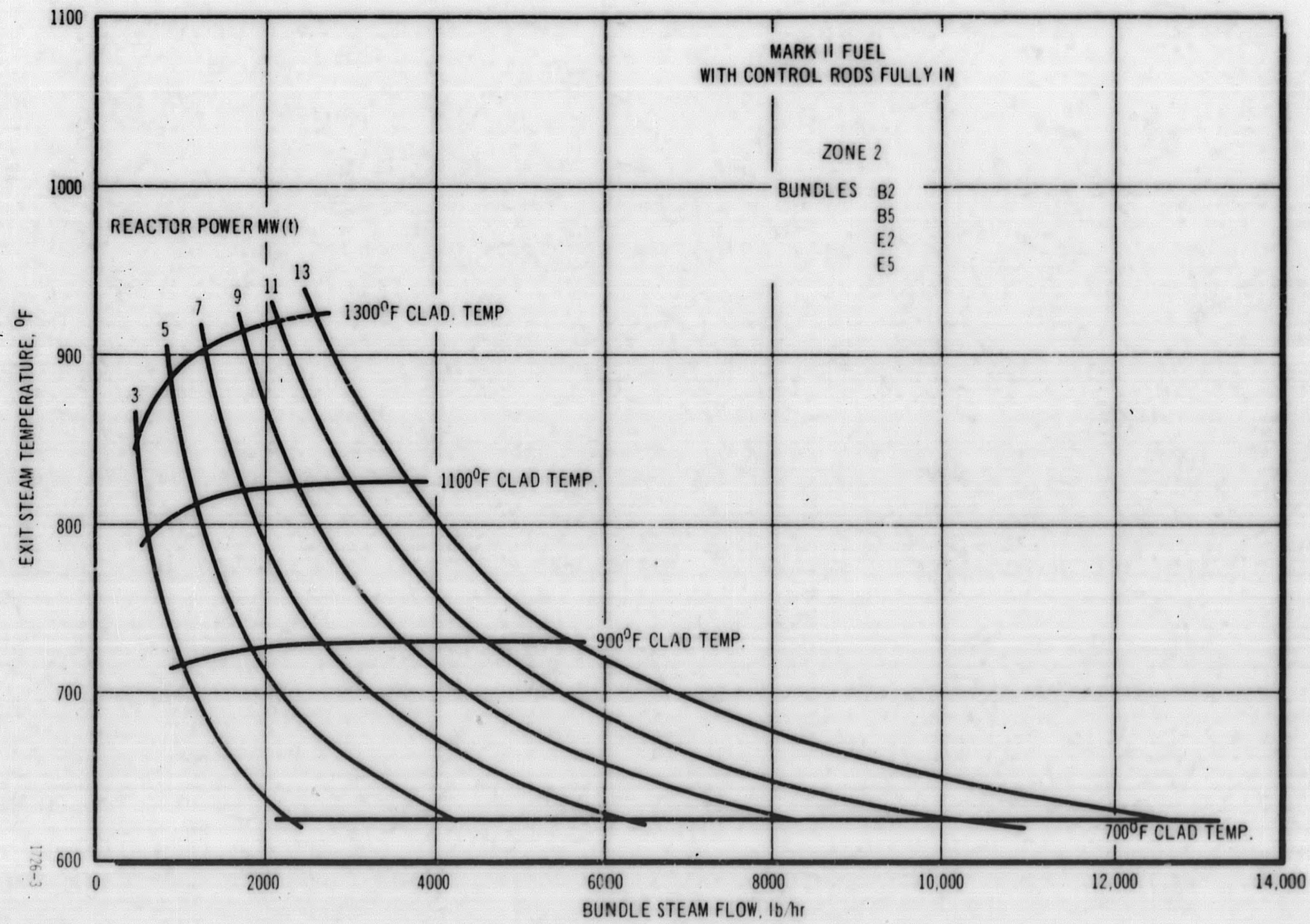


Figure 13-2. EVESR Mark II Fuel Operating Parameters

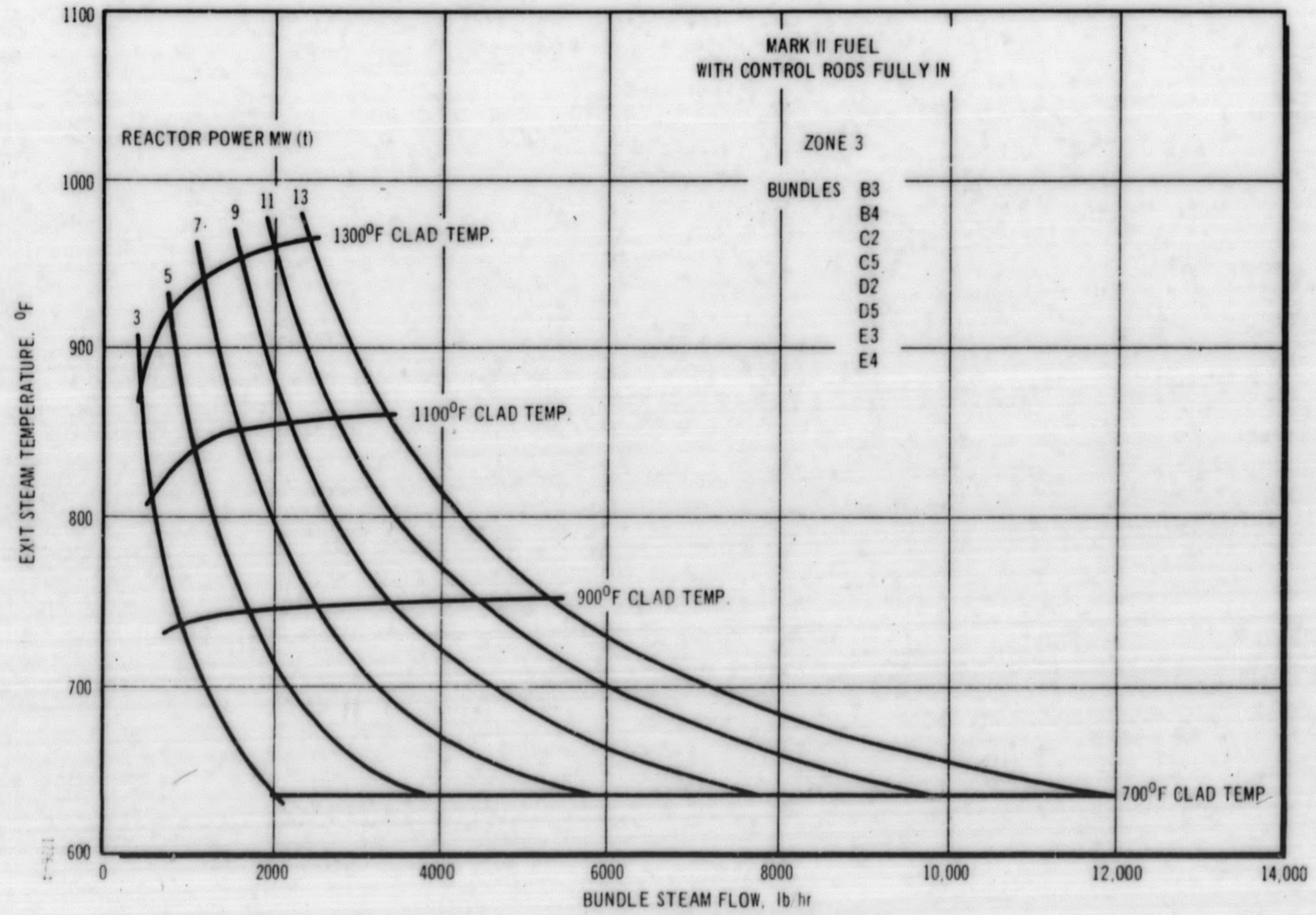
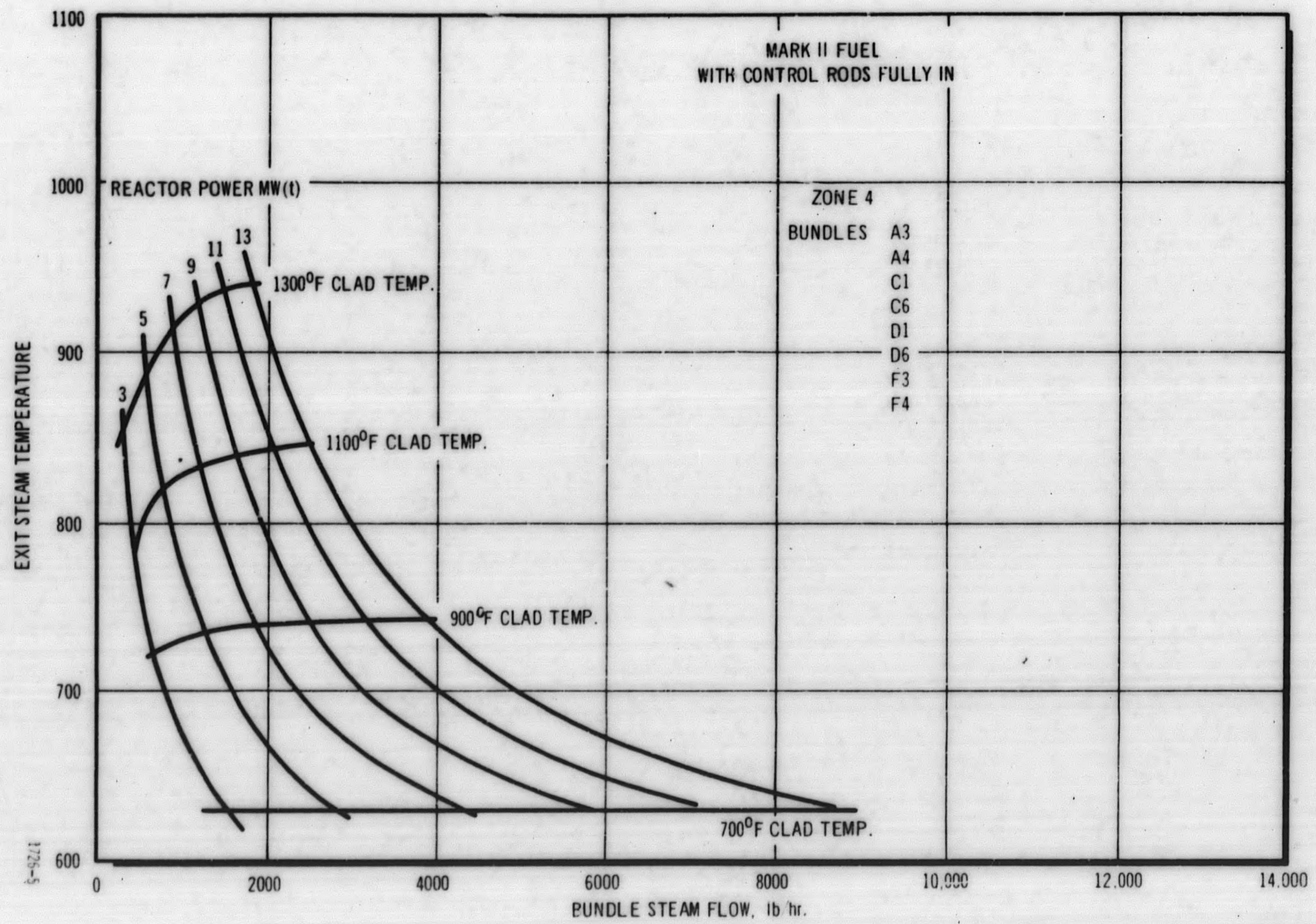


Figure 13-3. EVESR Mark II Fuel Operating Parameters



13-5

Figure 13-4. EVESR Mark II Fuel Operating Parameters

GEAP-4566

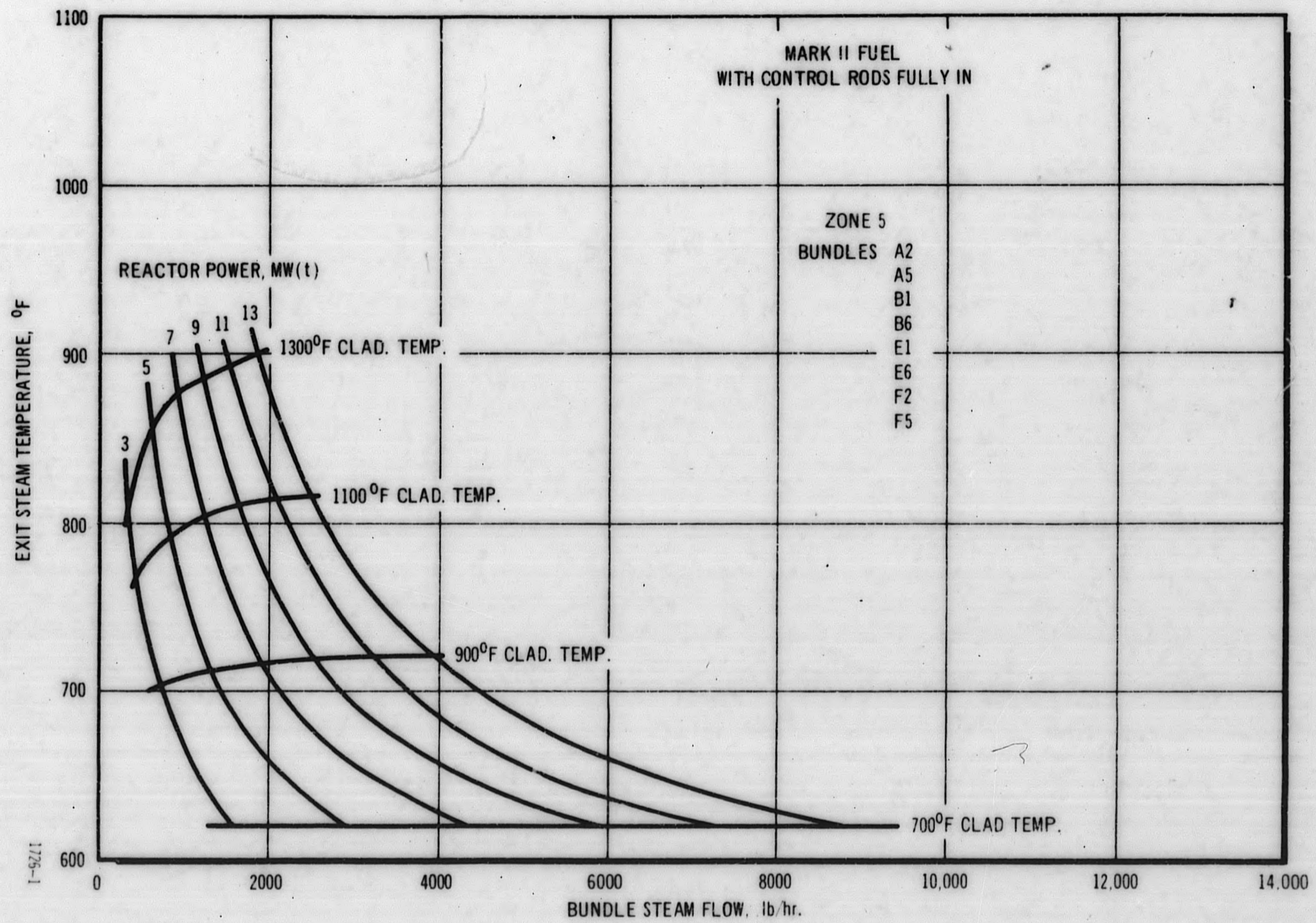


Figure 13-5. EVESR Mark II Fuel Operating Parameters

TABLE 13-1

Bundle Number	C4	B5	B4	A4	A5
Reactor Zone Number	1	2	3	4	5
Bundle Power Factor	1.216	1.128	1.162	0.870	0.796

Reactor Power MWt	Average Bundle Power (Btu/hr)	Bundle Power Btu/hr				
		C4	B5	B4	A4	A5
3	$0.319875 \times 10^6$	$0.38897 \times 10^6$	$0.36082 \times 10^6$	$0.37969 \times 10^6$	$0.278291 \times 10^6$	$0.254620 \times 10^6$
5	$0.533125 \times 10^6$	$0.64828 \times 10^6$	$0.60137 \times 10^6$	$0.61949 \times 10^6$	$0.463819 \times 10^6$	$0.42437 \times 10^6$
7	$0.746375 \times 10^6$	$0.90759 \times 10^6$	$0.84191 \times 10^6$	$0.86729 \times 10^6$	$0.649346 \times 10^6$	$0.49411 \times 10^6$
9	$0.959625 \times 10^6$	$1.1669 \times 10^6$	$1.08246 \times 10^6$	$1.11508 \times 10^6$	$0.834874 \times 10^6$	$0.776386 \times 10^6$
11	$1.172875 \times 10^6$	$1.42622 \times 10^6$	$1.323003 \times 10^6$	$1.36288 \times 10^6$	$1.02040 \times 10^6$	$0.93361 \times 10^6$
13	$1.386125 \times 10^6$	$1.68553 \times 10^6$	$1.56355 \times 10^6$	$1.61068 \times 10^6$	$1.20593 \times 10^6$	$1.10336 \times 10^6$

TABLE 13-2  
INPUT DATA FOR ZONE 1 BUNDLE C4

BPF = 1.216  
 ODI = 1.69  
 TMX = 1100.0  
 QF = 0.38897 \* 6  
 DPI = 1.29656 \* 6  
 RF(1) = 0.99, 1.01, 0.93, 1.02, 1.01, 1.01, 1.02, 1.02, 0.99  
  
 SKA(1.1) = 0.09 \* 9                      SKB(1.1) = 0.05 \* 9  
 SKA(1.2) = 0.07 \* 9                      SKB(1.2) = 0.04 \* 9  
 SKA(1.3) = 0.10 \* 9                      SKB(1.3) = 0.06 \* 9  
 SKA(1.4) = 0.08 \* 9                      SKB(1.4) = 0.04 \* 9  
 SKA(1.5) = 0.07 \* 9                      SKB(1.5) = 0.04 \* 9  
 SKA(1.6) = 0.07 \* 9                      SKB(1.6) = 0.04 \* 9  
 SKA(1.7) = 0.12 \* 9                      SKB(1.7) = 0.07 \* 9  
 SKA(1.8) = 0.08 \* 9                      SKB(1.8) = 0.04 \* 9  
 SKA(1.9) = 0.09 \* 9                      SKB(1.9) = 0.05 \* 9  
  
 FA(1.9) = 0.645, 0.985, 1.265, 1.395, 1.405, 1.285, 1.115, 0.865, 0.595, 0.445  
  
 MIT = 15                                      TAA = 150.0  
 MAXI = 15                                    TABV = 530.0  
 M = 9                                        ETC = 10.0  
 N(1) = 10 \* 8                              Z(1) = 1.25 \* 8  
 HCA(1) = 0.0                              XB = 0.97  
 HCB(1) = 0.0                              HGA(1) = 1000.0 \* 8  
 HGB(1) = 300.0 \* 8                       RCP = 1.0  
 DPCR = 0.84                               TCK = 10.0  
 ERRP = 0.1                                ERRT = 1.0  
 P = 975.0                                 TAI(1) = 545.0 \* 8  
 PER = 0.50                                TW(1) = 545.0 \* 8  
 EW = 10.0                                 WT = 570.0  
 RDP = 0.50                                TXT = 920.0  
 TAC = 900.0                               TBI(1) = 920.0 \* 8  
 TCK = 15                                    MP = 6  
 FE(1) = 0.0, 0.5, 0.5, 0.5, 0.5, 0.5, 0.5, 0.0, 0.5



TABLE 13-2 (Continued)

DA(1) = 1.346 * 8	DB(1) = 0.662 * 8	DP(1) = 1.474 * 8
DV(1) = 0.514 * 8	THA(1) = 0.028 * 8	THB(1) = 0.028 * 8
THP(1) = 0.028 * 8	CLK(1) = 12.0 *	FK(1) = 1.60 * 8
PTK(1) = 11.5 * 8	EC(1) = 0.5 *	EPT(1) = 0.5 * 8
AD(1) = 1.083-2 * 8	BD(1) = 1.242-2 * 8	AB(1) = 9.549 * 8
AA(1) = 1.999-3 * 8	AC(1) = 0.197-1 * 8	AN(1) = 0.800 * 8
AM(1) = 0.600 * 8	AU(1) = 0.575 * 8	AK(1) = 1.20 * 8
BC(1) = 0.197-1 * 8	BN(1) = 0.800 * 8	BM(1) = 0.600 * 8
BU(1) = 0.575 * 8	BK(1) = 0.600 * *	
QT = 0.937594 + 6	DPP = 0.77936 + 6	MP = 4
WT = 1800.0		

TABLE 13-3

DARE SYSTEM INPUT VARIABLE NAMES

<u>Symbol</u>	<u>Dimension</u>	<u>Definition</u>
AA	9	First Pass Flow Area
AB	9	Second Pass Flow Area
AC	1	First Pass Nusselt Coefficient - C
AD	9	First Pass Hydraulic Diameter
ADR	1	Radial Power Factor Normalization Check
AK	1	First Pass Nusselt Coefficient - K
AK1	1	First Pass Reynolds Number Coefficient - K1
AK2	1	First Pass Reynolds Number Coefficient - K2
AKL	20, 9	First Pass Pressure Loss Coefficients
AM	1	First Pass Nusselt Coefficient - M
AN	1	First Pass Nusselt Coefficient - N
AN1	1	First Pass Reynolds Number Coefficient - N1
AN2	1	First Pass Reynolds Number Coefficient - N2
AU	1	First Pass Nusselt Coefficient - U
BC	1	Second Pass Nusselt Coefficient - C
BD	9	Second Pass Hydraulic Diameter
BK	1	Second Pass Nusselt Coefficient - K
BK1		Second Pass Reynolds Number Coefficient - K1
BK2	1	Second Pass Reynolds Number Coefficient - K2
BKL	20, 9	Second Pass Pressure Loss Coefficients
BM	1	Second Pass Nusselt Coefficient - M
BN	1	Second Pass Nusselt Coefficient - N
BN1		Second Pass Reynolds Number Coefficient - N1
BN2	1	Second Pass Reynolds Number Coefficient - N2
BU	1	Second Pass Nusselt Coefficient - U
CLK	9	Clad Conductivity
CVP	1	Convergence Parameter - Pressure Loop
CVT	1	Convergence Parameter - Thermal Loop
DA	9	First Pass Clad Diameter (outside)
DB	9	Second Pass Clad Diameter (outside)
DBP	1	Change in Bundle Power (DARE 56)
DP	9	Process Tube Diameter (inside)
DPCR	1	Pressure Drop Guess Through Header (CORET)
DV	9	Velocity Booster Diameter (outside)
EC	9	Emissivity of The Cladding
EL	1	Fuel Length

TABLE 13-3 (Continued)

<u>Symbol</u>	<u>Dimension</u>	<u>Definition</u>
ELN	9	Length of Header Section (CORET)
EPT	9	Emissivity of the Process Tube
EQL	9	Equivalent Length of Header Section (CORET)
ERRP	1	Convergence Parameter For Pressure (DARE 5)
ERRT	1	Convergence Parameter For Temperature (DARE 5)
ETC	1	Convergence Parameter For Maximum Clad
EW	1	Convergence Parameter For Total Bundle Steam Flow
FA	20, 9	Axial Power Factor
FE	9	Material Emissivity Factor (CORET)
FK	9	Fuel Conductivity
FLA	9	Hydraulic Flow Areas (CORET)
HCA	9	First Pass Crud Conductance
HCB	9	Second Pass Crud Conductance
HGA	9	First Pass Gap Conductance
HGB	9	Second Pass Gap Conductance
KB	1	Bundle Number
M	1	Number of Elements in Bundle
MAXI	1	Number of External Iterations (PATSE)
MIT	1	Number of Internal Iterations (PATSE)
MP	1	Number of Power Increments (DARE 5)
N	1	Number of Nodes Per Element
OD1	1	Orifice Diameter (CORET)
P	1	System Pressure
PA	1	Bundle Exit Steam Temperature
PD	8, 9	Pipe Diameters (CORET)
PDT	9	Equivalent Pipe Diameters (CORET)
PER	1	Coolant Mixing Factor
PK	6, 9	Piping Conductivities (CORET)
FLM	1	Percent Power Lost to Moderator (PATSE)
PTK	9	Process Tube Conductivity
PTM	1	Midpass Steam Temperature
QT	1	Total Power
RCP	1	Flow Coefficient (DARE 5)
RDP	1	Required Bundle Pressure Drop
RF	9	Radial Power Factor
RYN	1	Reynolds Number For Laminar Flow Division
SKA	20, 9	First Pass Skewing Factors
SKB	20, 9	Second Pass Skewing Factors

TABLE 13-3 (Continued)

<u>Symbol</u>	<u>Dimension</u>	<u>Definition</u>
TA1	9	First Pass Entrance Steam Temperature
TAA	1	Ambient Air Temperature Outside Pipe Gallery
TABV	1	Moderator Inlet Temperature at Bottom of Fuel Bundles
TAC	1	Bundle Exit Steam Temperature
TB1	9	Second Pass Exit Steam Temperature
TCK	1	Maximum Clad Temperature Convergence Parameter
THA	9	First Pass Clad Thickness
THB	9	Second Pass Clad Thickness
THP	9	Process Tube Thickness
TMP	1	Average Mid-Pass Steam Temperature
TMX	1	Maximum Clad Temperature Allowed
TW	1	Sink Temperature
TXT	1	Average Exit Steam Temperature
WA	1	Bundle Flow Rate (DARE 5)
WT	1	Total Bundle Flow Rate
XB	1	Inlet Steam Quality (CORET)
Z	9	Power Ratio at Fuel Surfaces

## 14.0 SUB-TASK D-5: FUEL TESTS, COOLANT CHEMISTRY AND FUEL ACTIVITY RELEASE

### 14.1 Specifications and Data Requirements

Small amounts of impurities in the steam coolant reaching the EVESR fuel probably will contribute significantly to the corrosion of fuel cladding. The chemistry variables of the steam reaching the fuel of greatest interest are the following: moisture content, chloride concentration, fluoride concentration, conductivity, pH, gas composition, and solids composition. To the extent that suitable instrumentation or analytical techniques are available, these variables will be routinely measured and reported. Recognizing the difficulty in measuring impurities in the steam coolant, measurements will also be made of impurity levels in the boiler water and moderator water. Since boiler water and moderator water is the source of steam entering the fuel, these measurements will provide an indirect measure of steam impurities.

Excessive impurities in the boiler water and moderator water may compromise fuel testing. Therefore, reactor power operation will not be attempted or continued if the following chloride and conductivity conditions are exceeded:

<u>System</u>	<u>Chlorides</u>	<u>Conductivity</u>
Boiler Water	0.5 ppm	5 micromho/cm
Moderator Water	0.1 ppm	1 micromho/cm

In addition, the water in the fuel storage pool should have a conductivity of less than 2 micromho/cm, and is contingent upon installation of a demineralizer in the pool clean-up system.

The requirements for chemistry and related data to be taken were specified. Data sheets were prepared for chemistry data applicable to computer storage, and code numbers for the various chemistry parameters have been assigned.

### 14.2 Sampling and Procedures

A schedule was established for routinely sampling various system streams. Daily sampling was initiated on January 13, 1964, and samples are analyzed by analytical chemistry. Chloride is measured on reactor water and moderator water samples taken daily. On a less frequent basis fluoride, silica, nitrate, iron, copper, nickel, chromium, and total solids are also measured. Some of these measurements are periodically being made on other streams such as the hotwell water, condensate demineralizer effluent, reactor demineralizer effluent, condenser makeup, and fuel storage pool.

### 14.3 Boiler Water Chemistry

During December 1963 the conductivity of boiler water varied from 0.3 to 2.5 micromho/cm, averaging about 1.5 micromho/cm. Dissolved oxygen concentration in the boiler water during the month was normally less than 0.02 ppm when the boiler was idle. During periods of steam

flow, the continuous addition of oxygen to the boiler with the feedwater resulted in higher dissolved oxygen levels (0.2 ppm). Chlorides were less than 0.04 ppm and silica varied from 0.2 to 2.0 ppm.

During the first half of January 1964 the boiler was shut down and drained for internal inspection. During the latter half of January the boiler was operated at a relatively low steam generation rate with the reactor being bypassed most of the time. The conductivity of the boiler water was about 0.8 micromho/cm shortly after operation started on January 13, 1964. The conductivity gradually decreased for the next 10 days, when a conductivity of about 0.1 micromho/cm was reached. Conductivity remained at this level until a 3-day period at the end of the month when the boiler was operated at a relatively high steam generator rate; the conductivity went to 0.3 micromho/cm. Chloride levels in the boiler water did not exceed 0.04 ppm during the month and were generally less than 0.02 ppm. Silica concentrations were generally low during the month although a concentration of 7.6 ppm (as SiO<sub>2</sub>) was observed during the 3-day period mentioned above.

During most of February the boiler was operated at relatively low steam generation rate with the reactor bypassed except for a few hours on February 14, 1964. Boiler water conductivity varied from 0.1 to 0.4 micromho/cm during operation. Chloride levels in the boiler water did not exceed 0.02 ppm and generally were less than 0.02 ppm. Silica concentrations in the boiler water varied during the month from 0.08 ppm to 5.1 ppm. The high silica was related to condensate demineralizer operation and is further discussed below.

#### 14.4 Moderator Water Chemistry

Reactor moderator water samples are available only if the reactor cleanup system is in operation. Operational difficulties in maintaining the proper water level in the reactor vessel precluded continuous operation of this system during the period covered by this report. Since the reactor was not at power, no impurity concentration would take place in the moderator water. Infrequent measurements indicate that during December 1963 the conductivity of this water was less than 1.0 micromho/cm and chloride was less than 0.04 ppm. During January and February 1964 conductivity varied from 0.1 to 0.5 micromho/cm while the chloride was less than 0.04 ppm.

#### 14.5 Condensate Demineralizer Effluent Chemistry

The conductivity of the condensate demineralizer effluent during December 1963 varied from 0.08 to 0.6 micromho/cm and averaged about 0.2 micromho/cm. The conductivity observed was higher than expected and may be associated with higher than normal impurity levels in the hotwell discussed below. Conductivity breakthrough of the demineralizer was observed on December 27, 1963, and a new bed was placed in service. A sample of condensate demineralizer effluent taken from the old bed just before being taken out of service had a chloride concentration of 0.04 ppm and a silica concentration of 9 ppm.

The condensate demineralizer was not in service during the early part of January 1964 because of the boiler outage. During the last half of the month conductivity varied from 0.06 to 0.44 micromho/cm, and averaged 0.14 micromho/cm. During February the conductivity of this stream varied from 0.05 to 0.09 micromho/cm, averaging 0.07 micromho/cm. Chlorides in this stream during this report period was less than 0.04 ppm. Silica concentration in this stream was about 0.06 ppm on January 13 and this gradually increased to 1.7 ppm on February 12 when the standby demineralizer was put into operation. Within a few days the silica concentration in the condensate demineralizer effluent dropped to less than 0.01 ppm. On February 17 the old demineralizer was again put in service and by February 24, when the pressure drop across the bed became excessive, the silica concentration reached a maximum of 3.1 ppm. After the standby unit was again placed into service, the silica concentration dropped to less than 0.01 ppm. Changes in silica concentration in the boiler water followed the changes in condensate demineralizer effluent water silica concentrations.

#### 14.6 Hotwell Water Chemistry

The conductivity of hotwell water was higher than normal during early December 1963 (2 to 5 micromho/cm) indicating a leaking condenser tube. On December 19 the condenser was shutdown and one defective tube was found and plugged. During the remainder of this report period conductivity of hotwell water remained below 1 micromho/cm.

#### 14.7 Chemistry of Other Streams

On January 2 the conductivity of condenser makeup water was found to be about 90 micromho/cm, and a laboratory analysis of this water indicated a chloride concentration of 8.4 ppm, silica concentration of 4.4 ppm, and fluoride concentration of 0.05 ppm. The inability of the makeup demineralizer to maintain high purity water caused the abnormal condition. The resins in this demineralizer appeared to be fouled by organic impurities. Immediate replacement of this resin allowed water having adequate quality to be produced.

The pH of the various sample streams available at the condenser building sample station was measured in an open beaker. The measurements made indicate that the pH of all the streams was generally less than 7. The lowest pH values were observed in condensed boiler saturated steam in which the pH reached a low of 5.6. The low values were observed during transient conditions with low steam generation rates. The technique used is sufficiently rapid to avoid pH lowering of the sample because of contamination by atmospheric carbon dioxide; however, to completely avoid the problem of sample contamination a closed sampling and measuring system must be used.

#### 15.0 SUB-TASK E-1 AND E-2: FUEL EXAMINATIONS

A vertical orientation has been selected over horizontal positioning for cutting and examining EVESR fuel bundles in the fuel storage pool. This selection was made possible by the choice of a telescope rather than a periscope for viewing the underwater portions of irradiated fuel bundles. The telescope can be focused to view at any depth along the vertically positioned fuel bundle; while a periscope would be designed to view at only one depth and would require the fuel bundle to be laid horizontally. The vertical positioning will eliminate the need for a tilt table and will simplify handling of fuel bundles in the pool.

The telescope for underwater viewing of fuel elements was received and a simulated examination was made of the dummy fuel element in air. This demonstrated the need for a very solid mount and the design has been oriented accordingly. Conceptual design of associated examination equipment is essentially complete. More tests are scheduled in the pool.

Drawings have been completed for the underwater saw and the fuel element storage cans. A prototype can will be constructed and tested during March.

The prototype cut fuel bundle storage channel was installed in the storage rack. A successful check was made by installing the cut dummy fuel bundle in the new rack. Fourteen additional channels are being fabricated and are expected to be installed next month.

Drawings for the leak testing equipment were also completed, and fabrication will proceed in March.



## 16.0 TASK F: NUCLEAR SUPERHEAT FUEL DEVELOPMENT PROGRAM

### 16.1 Objectives

The objective of the EVESR Nuclear Superheat Fuel Development Program is to establish minimum performance levels and to demonstrate satisfactory performance of superheat fuel elements that will produce competitive power when irradiated in reactors with large enough power output to be of economic interest. As part of this objective, it is expected that knowledge and understanding of performance and endurance limits will be developed as necessary to provide a technical basis for design of superheat fuel elements in large commercial power reactors.

The program is based on three fundamentally different types of fuel performance evaluations for two fundamentally different reactor applications. The three types of fuel evaluations are:

- a. Cladding performance evaluation to establish, on an accelerated basis, an ordering of preference of cladding materials. This will involve irradiation of Inconel, Incoloy, high purity Type 310 stainless steel, high purity Type 304 stainless steel, and commercial Type 304 stainless steel, as fabricated in the Mark II fuel configuration. The high cladding stress levels and severe operating conditions associated with the large diameter Mark II annular fuel configuration are expected to result in early determination of the performance limits of the various cladding materials being evaluated. It is expected that information from the Mark II fuel irradiation will be of significant value in extrapolating the life of fuel cladding used in the more economic, small-diameter rod fuel geometry.
- b. Demonstration of high heat flux, high power density performance in fuel elements operating at the maximum burnup capability of the EVESR facility. The programmatic objective of these irradiations will be to install seven-rod cluster, thermal superheat, rod geometry fuel elements and mixed spectrum rod fuel elements in the reactor as early as possible in order to achieve the maximum burnup at high levels of heat flux and specific power. This program objective will be achieved by insertion of Mark III and Mark IV fuel elements into the high worth positions in EVESR at the earliest time consistent with minimum development features, for a meaningful fuel irradiation. In the case of the Mark IV MSSR designs, it may be necessary to increase clad thickness to provide a closer simulation of expected clad stresses at MSSR operating conditions. This requirement results from differences in thermal and fast flux environments.
- c. Mechanical performance evaluation of economically optimized fuel configurations such as seven-rod cluster, thermal superheat fuel elements, and mixed spectrum fuel elements. Irradiation of these Mark V and Mark VI fuel elements will be delayed to permit incorporation of those features established on the basis of development work during the first year of the program. The objective of this development work will be to investigate fuel features having the potential to provide significant reductions in cost of power.

Examples of development work areas for economic optimization are thin Zircaloy process tubes, improved fabrication techniques, improved heat transfer features, and cladding material and design basis. Since the objective of the previous irradiation (paragraph b) is high burnup and high heat flux, Mark III and Mark IV elements will utilize the high performance positions. Therefore, the value of the operating experience obtained from irradiation of Mark V and Mark VI fuel elements is based on the ability to separate between the performance limits associated with high specific power and high fuel metal temperatures. This is a reasonable objective since all conditions external to the outer fiber of the fuel clad may be simulated by adjusting the coolant flow to the desired clad surface temperature.

In addition to the three fundamental types of fuel evaluations listed above, fuel for two basic reactor applications will be evaluated as part of the EVESR program. These are the seven-rod cluster, rod type fuel elements for application in either integral or thermal superheat reactors, and the small-diameter rod characteristic of the high heat flux, high specific power fuel in the fast spectrum, superheat region of the mixed spectrum superheat reactor.

TABLE 16-1  
PRELIMINARY PLAN FOR ADVANCED FUEL PROGRAM

Designation	Fuel Geometry	Program Objective	Estimated Time for Installation	Position in EVESR	Element Removed	Predicted Performance with 135,000 lb/hr Steam Flow				Program Details		
						Normal Control Rod Pattern	Reversed Rod Pattern	Design Maximum Clad Temperature	Burnup at September 1966 60% Load Factor	Spacer	Process Tube	Key Features
Phase I 32 Mark II	0.028 inch clad, 1-1/4 inch OD by 3/4 inch ID - Incoloy, Inconel, 310 VM, 304 VM, and Comm. 304	Evaluate fuel clad performance	November 1963	Initial load	Not applicable	9 kW/kg at 110,000	-	1250	4,000 average	Dimpled process tube	Uninsulated stainless steel	-
Phase II 28 Mark II 4 Mark III	(Mark III) four required 0.455 inch OD by 5 foot seven-rod cluster Incoloy 0.008 - 0.020 clad	1) Maximum burn-up 2) Effect of clad thickness 3) Minimum development economic features	July 1964	four central locations C-3 C-4 Zone 1 D-3 D-4	Mark II one - 304 Comm. three - 304 VM	13 kW/kg at 100,000	34 kW/kg at 260,000	1250	≈ 8000 MWD/T 50 percent Eff at 34 kW/kg	Spiral Wire	Zircaloy-2 with mechanical joint	Standard UO <sub>2</sub> pellets 1 to 3 mil swaged, 0.030 liner, scallop type
Phase III 25 Mark II 4 Mark III 2 Mark IV 1 ESH-3	(Mark IV) two 0.25 inch OD by 5 foot seven-rod cluster Incoloy, Inconel  ESH-3	1) Maximum burn-up MSSR prototype (Minimum Development)  2) Continue ESH 1.1 burnup	September 1964	C-2 } Zone 3 B-3 }	Incoloy 1100°F	15 kW/kg at 60,000	~ 50 kW/kg at 180,000	1250	550 MWD/T 50 percent Eff based on 20 kW/kg	Spiral Wire	Stainless steel scalloped liner, uninsulated	1/4 inch diameter - seven-rod cluster
	September 1964		B-2 Zone 2	1250°F 310 VM	As above.	13 kW/kg at 100,000	34 kW/kg at 260,000 except C-3 down 15 percent	1250		As per ESH-3	As per ESH-3	
	Already in: Mark III (four)  Mark II (25)			C-3 C-4 Zone 1 D-3 D-4		9 kW/kg at 110,000	11.5 kW/kg	1250				

TABLE 16-1  
(continued)

Designation	Fuel Geometry	Program Objective	Estimated Time for Installation	Position in EVESR	Element Removed	Predicted Performance with 135,000 lb/hr Steam Flow				Program Details		
						Normal Control Rod Pattern	Reversed Rod Pattern	Design Maximum Clad Temperature	Burnup at September 1966 60%	Spacer	Process Tube	Key Features
<p><u>Phase IV</u></p> <p>21 Mark II 4 Mark III 2 Mark IV 4 Mark V 1 ESH-3</p>	<p>Mark V - four required 0.45 inch CD by 5 foot</p> <p>two Hastelloy-X .012 .020 .012 .020</p> <p>two Incoloy .020</p> <p>Mark IV - two</p> <p>ESH-3 - one</p> <p>Mark III - four</p> <p>Mark II - 21</p>	<p>1) Optimized performance seven-rod cluster thermal SH</p> <p>2) High temperature effect</p> <p>3) Separate effect of liners and spacers</p> <p>4) Test swaged powder fuel</p>	January 1965	<p>B-1 C-1 Zone 4 D-1 and 5 E-1</p> <p>C-2, B-3</p> <p>B-2</p> <p>C-3, C-4 D-3, D-4</p>	<p>1100° F Inconel 1100° F Inconel 1100° F Incoloy 1100° F Incoloy</p>	<p>10 kW/kg at 80,000</p> <p>12 kW/kg at 50,000</p> <p>13 kW/kg at 100,000</p>	<p>7 kW/kg at 50,000</p> <p>18 kW/kg at 75,000</p> <p>34 kW/kg at 260,000</p> <p>C-3 down 15 percent</p>	<p>1250 (2) 1400 (2)</p> <p>1250</p> <p>1250</p>	<p>≈ 2300 MWD/T 80 percent Eff at 7 kW/kg</p>	<p>Dimpled spacer on fuel clad, spring type or other non-spiral wire spacer</p>	<p>Thin Incoloy Liner, Zirc-Incoloy Metallurgical joint</p>	<p>1) Swaged powder improved heat transfer</p> <p>2) UO<sub>2</sub> pellets (1-3 mil gap light swage) Test one each at high temperature</p>
<p><u>Phase VA</u></p>	<p>GNEC - two Comb. Boiling Superheat Mark V - four Mark III - four Mark IV - two ESH-3 one Mark II - 19</p>	<p>Eval. comb. boil-SH for BONUS II</p>	July 1965	<p>E-2 E-5</p>	<p>1250 310 VM 1250 310 VM</p>	<p>5 kW/kg 225,000 Same as Phase IV</p>	<p>3.5 kW/kg 155,000 Same as Phase IV</p>					

TABLE 16-1 (continued)

Designation	Fuel Geometry	Program Objective	Estimated Time for Installation	Position in EVESR	Element Removed	Predicted Performance with 135,000 lb/hr Steam Flow				Program Details			
						Normal Control Rod Pattern	Reversed Rod Pattern	Design Maximum Clad Temperature	Burnup at September 1966 60% Load Factor	Spacer	Process Tube	Key Features	
Phase V	Mark VI - four	Optimized performance MSSR, 13-rod cluster	July 1965	B-4, D-2 C-5, D-5	1250 Incoloy 1250 Incoloy	10 kW/kg 45,000	15 kW/kg 70,000		2500 MWD/T at 80 percent eff. at 15 kW/kg				
	Mark V - four					8 kW/kg 60,000	6 kW/kg 50,000						
	Mark IV - two					10 kW/kg 45,000	15 kW/kg 70,000						
	ES 1-3 - one												
	Mark III - four					11 kW/kg 90,000	23 kW/kg 180,000						
Mark II - 17		7 kW/kg 85,000	9 kW/kg two bundles E-3 at E-4										
													Remaining Mark II six - 1250 Incoloy two - 1100 Incoloy one - 310 VM six - 1250 Inconel two - 1100 Inconel <hr/> 17

## 17.0 SUB-TASK F-1: ADVANCED FUEL, GENERAL DEVELOPMENT

### 17.1 High Temperature Autoclave Testing of Fuel Capsules

The EVESR Advanced Fuel Program consists of designing and testing fuel assemblies which have the objectives of demonstrating long-life and competitive economic performance. To meet the economic objectives of the program, it is necessary to progress to thin-clad fuel designs where instability collapse will occur unless sufficient support is given to the clad by the fuel column. The factors leading to instability collapse are:

- a. Initial gap between fuel and cladding,
- b. Strength of cladding,
- c. Powder or pellet type fuel, and
- d. Ovality and thickness variation of tubing used.

To relate the various factors leading to instability collapse, a program has been initiated to determine the mechanical creep and wrinkle formation characteristics of the various fuel designs contemplated for the advanced fuel program. The testing will be conducted in a horizontal autoclave operating at 1200°F and 1000 psi. Both pellet- and powder-filled capsules will be tested with sheath wall thickness varying from 8 to 20 mils. The tests will be performed in increments of 100 hours for a total of 1000 hours for each specimen. After each 100-hour run, the capsules will be examined and measured to detect wrinkle formation or depressions at pellet interfaces.

The testing of the first group of 12 capsules, whose characteristics are shown in Table 17-1, has begun. The design for the second group of 12 capsules has been completed and procurement of materials is in progress.

### 17.2 Heat Transfer Tests

The heat transfer tests being carried out under this task are directed toward studying the effects of fuel element geometry and power distribution. The test section for this study consists of an "infinite" array of 1-inch diameter rods with a 20-inch unheated entrance length and 40-inch heated length. The first series of tests is for a pitch-to-diameter ratio of 1.25. Heat transfer tests have been run with this test section over the Reynolds number range of 20,000 to 200,000. Preliminary examination indicates that the data is consistent within itself, satisfactorily correlating wall-to-bulk temperature differences and density change, by virtue of pressure variation, up to eight times.

Heat flux variation around the periphery of a flow duct has a greater influence on wall temperature variation than previously supposed. The problem was first solved for the case of a circular tube, <sup>(5)</sup> where it was shown that the wall temperature variation could be appreciable, even for turbulent flow. Because peripheral heat flux variation occurs in reactor fuel elements by virtue of the skewing of neutron flux distribution across the element, this problem is of interest for

reactor fuel element geometries. A digital computer was used to solve the turbulent flow equations for annuli with radius ratios from 0 to 0.9; Reynolds numbers of  $10^4$ ,  $10^5$ , and  $10^6$ ; and over a Prandtl number range of 0.01 to 10. A report <sup>(6)</sup> covering the results of this work has been prepared and is being issued.

### 17.3 Stress Corrosion Cracking of Superheat Fuel Sheathing

Five different alloys are being used for fuel sheathing and include Type 304 commercial grade stainless steel, Types 304 and 310 vacuum melt stainless steel, Incoloy, and Inconel. One failure mechanism which might limit the life of one or more of these alloys is the highly-localized corrosion attack known as stress corrosion cracking. It is well known that the 300 series austenitic stainless steels are susceptible to stress corrosion cracking, and that resistance can be improved by decreasing nitrogen content and increasing the nickel content; therefore, one would expect increasing resistance to stress corrosion cracking in the order listed above.

As part of an overall alloy evaluation program for superheat applications, a program was initiated to determine, quantitatively, the relative resistance of these alloys to stress corrosion cracking in boiling 42 weight percent magnesium chloride. The purpose of this section is to report the results obtained as of February 15, 1964.

#### 17.3.1 Specimen Preparation and Test Procedure

The material used for preparing the corrosion specimens was excess tubing from the Mark II fuel fabrication. The chemical composition and typical tensile properties of the five alloys are shown in Table 17-2. The specimens were prepared from tubing by shearing a 1/4-inch wide by 6-inch long specimen from the tubing and then milling a tensile specimen as shown in Figure 17-1. The specimens are then polished to remove burns and disturbed metal from the milled surfaces. The finished specimens are inserted through openings in a glass reaction vessel. Specimen junctions are then sealed by an epoxy. Boiling 42 weight percent magnesium chloride is poured into the reaction vessel equipped with a reflux condenser and the corrosion test begins. A test in progress is shown in Figure 17-2.

The time-to-failure of a specimen is determined by a timer wired through a microswitch attached to the specimen loading mechanism. When the load is released, the timer is stopped and the indicated reading is the time-to-failure. It should be noted that this test is specimen size dependent since it includes the nucleation time, the crack propagation time, and the time required for the final ductile fracture which occurs when the reduced cross-sectional area can no longer sustain the load.

TABLE 17-1  
PRETESTING DATA FOR BUNDLE NUMBER 1

Material	Rod Number	Initial		Final		Wall Thickness (inch)	Type of Fuel	Percent Density	Annealed	Fuel-To-Clad Gap (inch)	Length (inch)	After Anneal OD (inches)	After Reswage OD inch
		OD (inch)	ID (inch)	OD (inch)	ID (inch)								
Incoloy	L-1	0.4518	0.4119	0.4518	0.4119	0.0199	Standard Pellet	95.6	No	0.005	10.310		
	L-2	0.4507	0.4178	0.4438	0.4114	0.0162	Swaged Pellet	95.6	Yes	0.004	10.360	0.4450	0.4430
	L-3	0.4507	0.4179	0.4507	0.4199	0.0161	Standard Pellet	95.6	No	0.002	10.295		
	L-4	0.4508	0.4181	0.4508	0.4181	0.0161	Standard Pellet	95.6	No	0.004	10.304		
	L-11	0.4512	0.4274	0.4512	0.4274	0.0119	Standard Pellet	95.6	No	0.002	10.307		
	L-12	0.4512	0.4274	0.4433	0.4195	0.0119	Swaged Pellet	95.6	Yes	0.003	10.372	0.4440	0.4428
	L-21	0.4516	0.4356	0.4516	0.4356	0.0082	Standard Pellet	95.6	No	0.002	10.311		
	L-22	0.4515	0.4357	0.4433	0.4275	0.0079	Swaged Pellet	95.6	Yes	0.003	10.370	0.4450	0.4425
	L-23	0.4515	0.4356	0.4433	0.4273	0.0080	Swaged Pellet	95.6	No	0.002	10.375		
	L-24	0.4515	0.4358	0.4435	0.4277	0.0079	Swaged Pellet	95.6	No	0.002	10.375		
	L-25	0.540	0.508	0.4460	0.4140	0.016	Swaged Powder	88	No	--	10.303		
Incoloy	L-26	0.540	0.508	0.4460	0.4140	0.016	Swaged Powder	88	Yes	--	9.923	0.4485	0.4450



TABLE 17-2

## TYPICAL CHEMICAL ANALYSIS AND TENSILE PROPERTIES OF EVESR MARK II FUEL SHEATHING

Alloy	Chemical Analysis (Percent)														Tensile Properties		
	Ni	Cr	C	Mn	P	S	Si	Mo	Ti	Co	Cu	Al	N	Fe	Yield Strength (0.2 percent offset) $10^{-3}$ psi	UTS $10^{-3}$ psi	Percent Elong- ation
Incoloy	33.4	20.8	0.06	1.1	0.005	0.006	0.65	-	0.05	0.02	0.03	0.05	0.06	Bal	47	93	39
Inconel	76.4	15.1	0.02	0.22	-	0.007	0.31	-	0.1	0.08	0.21	-	-	7.7	37	93	38
310 VM	20.2	25	0.003	1.02	0.003	0.003	0.42	0.06	-	-	-	-	0.008	Bal	37	79	45
304 VM	9.4	17.8	0.005	0.55	0.01	0.007	0.36	0.01	-	0.02	-	-	0.009	Bal	33	85	60
304 H	8.8	18.3	0.05	0.80	0.01	0.008	0.66	0.20	-	0.05	0.18	-	-	Bal	40	107	61



Figure 17-1. Tensile Specimen For Stress Corrosion Tests (~1.3X)

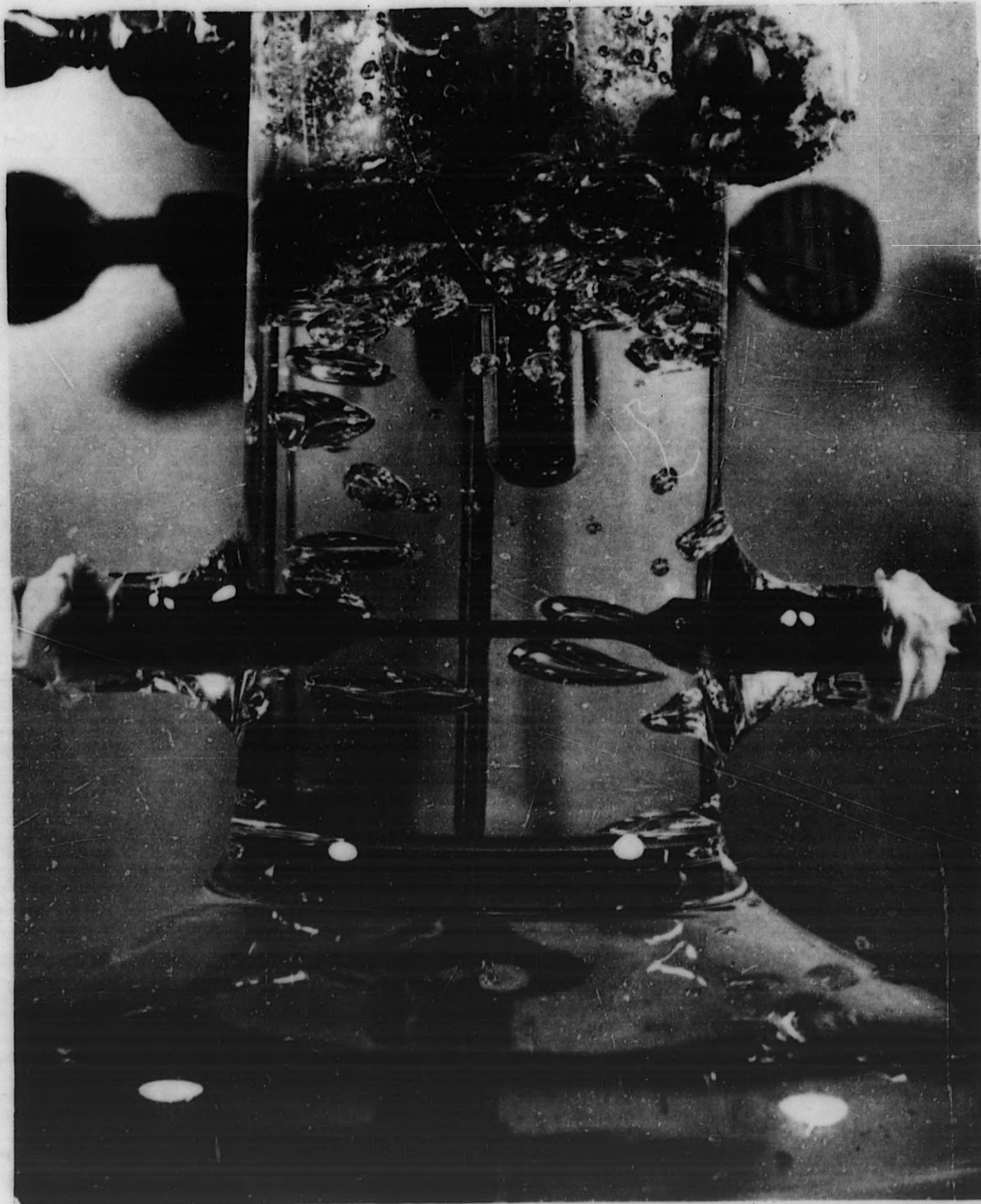


Figure 17-2. Corrosion Test in Progress. Solution is Boiling  
42 w/o MgCl<sub>2</sub>.

### 17.3.2 Results

The results obtained during this reporting period are shown in Figure 17-3 where stress has been plotted as a function of time-to-failure for each alloy. The order of increasing resistance is as expected from work reported in the literature. There is a knee in each curve which occurs approximately at the yield strength of each alloy which is in agreement with other investigators.

The relative resistance to cracking exhibited by the commercial grade and vacuum melt Type 304 stainless steel is particularly interesting. Above the yield strength of the materials very little benefit is gained by the vacuum melt material while below the yield point the time-to-failure is increased by an order of magnitude.

The Type 310 vacuum melt stainless steel is more resistant to cracking than the Type 304 stainless steel, indicating the beneficial results of higher nickel content, and then the Incoloy and Inconel. All tests were terminated at 40,000 minutes if failure had not occurred as indicated by the arrow in Figure 12-3. It is significant to note that the Type 310 VM specimen stressed at 20,000 psi, the Incoloy stressed at 50,000 psi, and the Inconel stressed at 70,000 psi did not fail.

Metallographic examination of the Type 310 VM specimen stressed at 20,000 psi has shown some crack penetration, as shown in Figure 17-4. The cracking is in the curved portion of the tensile specimen where some grain deformation from the milling operation is evident. Presumably the cracks nucleated in the curved region rather than the more highly stressed region because of the cold worked surface grains. Another series of tests is being performed with more careful polishing of the milled surface followed by etching.

### 17.4 Fuel Clad Strain Cycling

An analysis was undertaken to obtain an estimate of the relative strain-cycle performance of the various EVESR cladding materials. Strain cycling can be defined as low cycle fatigue, or as cladding plastic strain range, occurring because of changes in reactor operating power.

Wrinkling and corrosion, either of which will tend to reduce strain-cycle life, were not considered in the analysis.\* The analysis was completed during the quarter, and the results are outlined below.

For 12.5-MW operation, strain cycling is calculated to be negligible for all EVESR Mark II cladding materials. As burnup occurs, the core power distribution changes, resulting in increased strain cycling for nearly all materials. The worst case will occur at core mid-life, the results of which were tabulated in Table 17-3. The low strain-cycle life for the Type 304 VM stainless steel at core mid-life is due to:

\*Initial ovality was considered as discussed on page 10 of reference (7). The fuel specification called for 0.004-inch clad-to-fuel maximum gap to minimize the possibility of wrinkling.

17-5

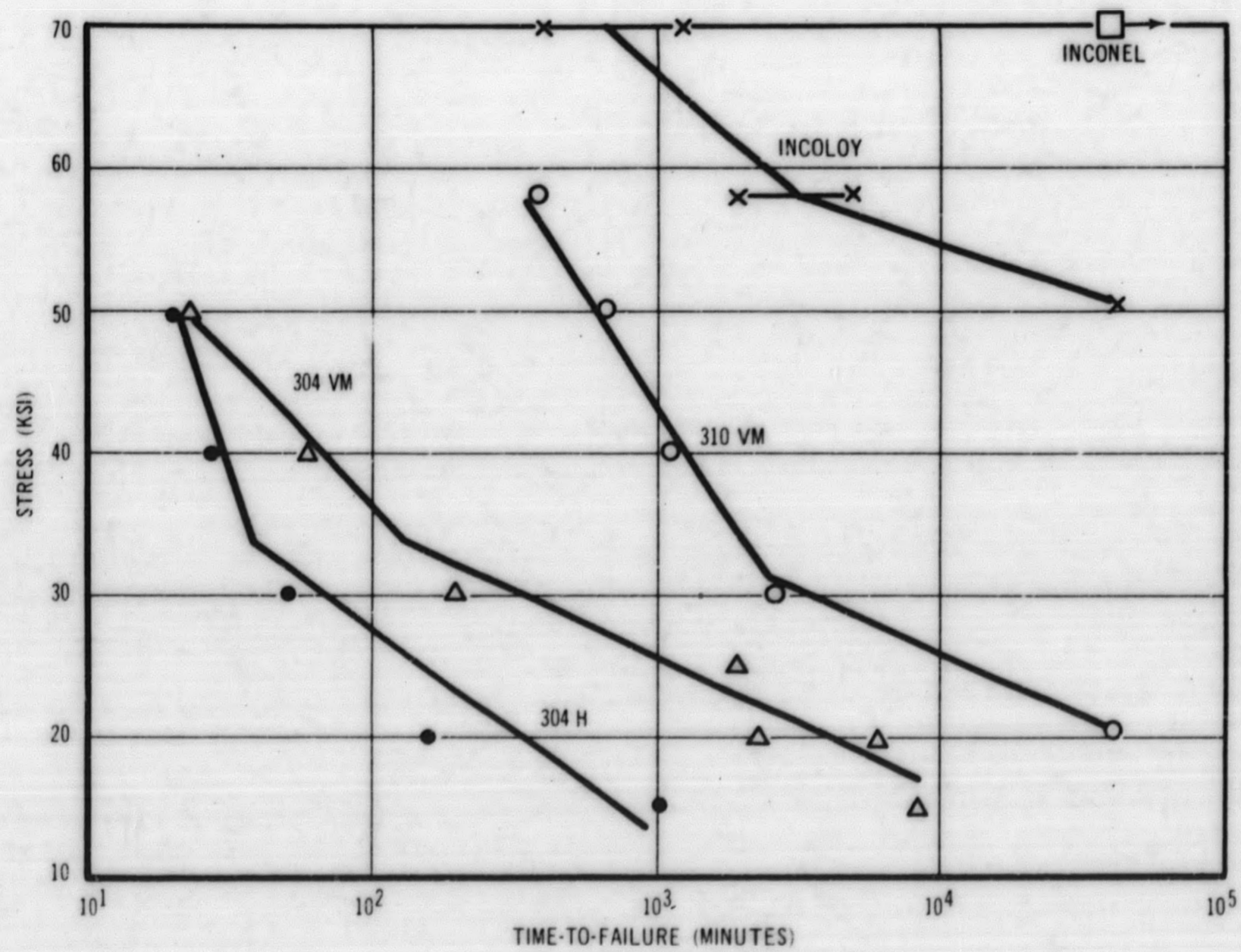


Figure 17-3. Stress Versus Time-To-Failure in Boiling 42 Weight Percent MgCl<sub>2</sub>

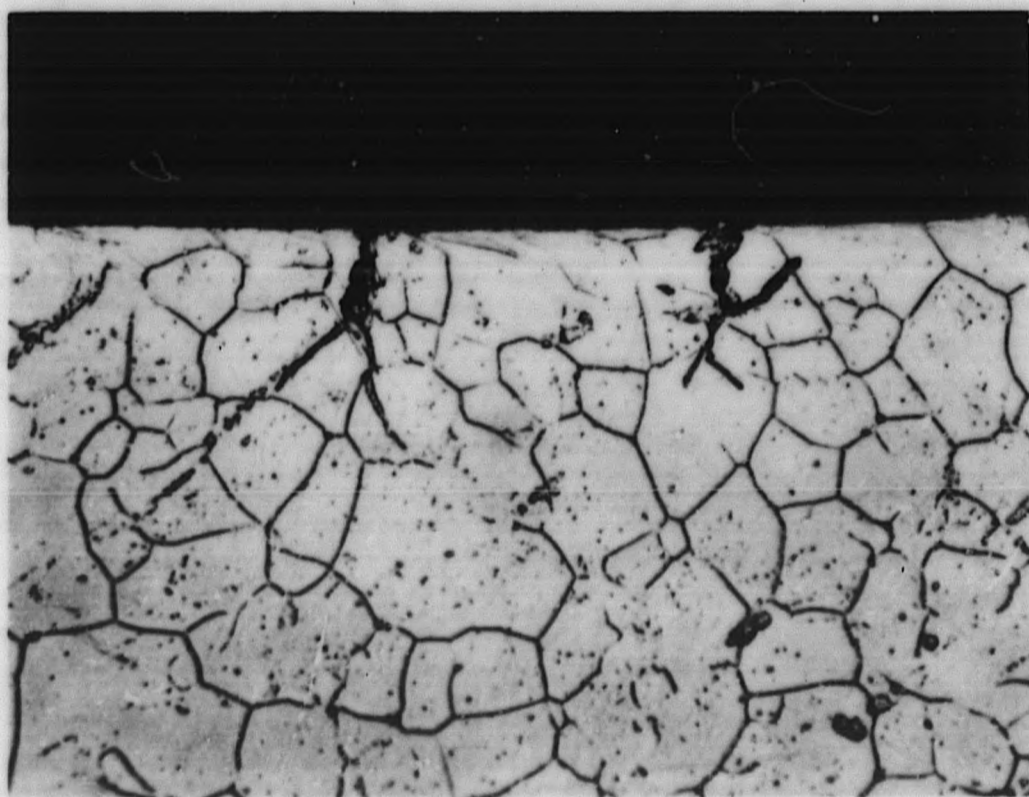


Figure 17-4. Macrograph of 310 VM Stainless Steel Test Specimen and Micrograph Showing Stress Corrosion Cracks

- a. Irradiation in the highest power part of the core, and
- b. Having low strength due primarily to low carbon content.

17.4.1 Conclusions

- a. If wrinkling were to occur, the strain cycling for any Mark II fuel clad material could result in even shorter strain-cycle life than is listed for the Type 304 VM stainless steel.
- b. Because of possible inaccuracies discussed below, the results presented here give general trends and not precise values.
- c. Strain-cycle performance of all Mark II materials except possible Type 304 VM stainless steel should be satisfactory, even if the unmodified\*\* Reynolds' data apply.
- d. If the modified† Reynolds' data apply, strain cycle performance, even of Type 304 VM stainless steel, should be satisfactory.

TABLE 17-3  
EVESR MARK II STRAIN CYCLING TRENDS

<u>Cycles to Failure</u>		
12.5-MW Mid-Life		
Reynolds' Data		
<u>Material</u>	<u>Unmodified**</u>	<u>Modified†</u>
Inconel	N.C.*	N.C.
Incoloy	N.C.	N.C.
310 VM	N.C.	N.C.
304 VM	150 to 500	> 1000
304 H	N.C.	N.C.

\*N.C. - Negligible Cycling

Note: Number of cycles has been reduced two-thirds to estimate radiation effects. Type 304 VM stainless steel is assumed to follow the same strain versus cycles curve as Type 304H stainless steel. Type 310 VM stainless steel is assumed to follow the Incoloy strain versus cycle curve.

\*\*Figure 5.1 - reference (7) - The unmodified data predict shortest strain-cycle life.

†Figure 5.2 - reference (7).

#### 17.4.2 Method

The displacement method of Rieger<sup>(7)</sup> was used in the strain-cycle analysis with two modifications: (1) instead of going immediately to the maximum-power point of the stress-strain hysteresis loop, the stress-strain curve was begun by first applying the external 1000 psi pressure and 600°F no-power conditions, and (2) an estimate was made of increased circumferential clad strain due to pellet ridging.<sup>(8)</sup> The operating condition was taken at the most probable clad temperature (1100°F), with shutdown at 600°F.

In addition to the assumptions of reference (7) (volumetric average fuel temperature applies for fuel expansion; uni-axial tensile stress-strain curve applies for both compressive and tensile cladding strain), the following assumptions were used:

- a. UO<sub>2</sub> surface heat flux (at the axial power peak) is equal for inner and outer passes.
- b. The thermal diffusion equation with constant UO<sub>2</sub> thermal conductivity and constant volumetric heat generation applies.
- c. The UO<sub>2</sub> thermal conductivity value at the volumetric average temperature applies.
- d. UO<sub>2</sub> thermal conductivity value of Lyons<sup>(9)</sup> and linear expansion coefficient of Burdick and Parker<sup>(10)</sup> apply.
- e. All power is generated in the fuel. This neglects the fact that about 5 percent of the power is generated directly in the moderator.<sup>(11)</sup>
- f. Fuel pellets have circumferential ridges at each end. The diametral height of a ridge is 0.0014 inch\* at a heat flux of 131,000 Btu/h-ft<sup>2</sup>, and ridge height is linear with heat flux.
- g. Outer clad-to-fuel gap conductance is 1000 Btu/h-ft<sup>2</sup>-°F. The effect of any inaccuracies introduced by assumptions a. through g. will be to change the amount of UO<sub>2</sub> expansion at power.
- h. Rate of change of radial heat flux with respect to axial distance is negligible at the peak power location.
- i. As-built clad-to-fuel diametral gap (room temperature) is 0.002-inch (minimum gap will be the amount of clad spring-back, about 0.0015 inch, due to pressurization during fabrication. Maximum allowed gap is 0.004 inch.
- j. Longitudinal effects of pellet ridging on cycling are negligible.
- k. Cladding does not restrict fuel expansion. (Interference stresses in the cladding will be much greater than in the fuel because of the high fuel-thickness-to-clad-thickness ratio.)
- l. There is no change in cladding stress-strain curve due to irradiation, cycling, thermal aging, etc.; that is, yield strength at arbitrary offset value does not change with time.
- m. The thinnest cladding is used at the highest power locations for each material.

\*This value of ridge height is estimated from work done by S. W. Tagart in 1962 for EVESR stress calculations.



Power distribution of reference (11) was used in the analysis except that a constant axial power peak of 1.8 was used for all materials.

17.4.3 Accuracy

Major sources of possible error in plastic strain are inaccuracies in (1) fuel element maximum power level relative to core average, (2) magnitude of UO<sub>2</sub>-to-clad relative expansion, and (3) material stress-strain curve -- both initially and as irradiation time increases. Assumptions a. to g. would affect error-source two, and should treat all materials the same. The other assumptions except 1. consider fuel geometry and also should treat all materials nearly the same. Assumption 1. would affect error-source three. This may be the greatest possibility for error. For example, most of the EVESR clad materials operate at stresses and strains between the linear part of the stress strain curve and the at-temperature yield point. In this region a 10 percent change in yield strength can permit a 300 percent change in plastic strain range for some operating conditions. Neutron irradiation usually acts to increase yield strength; strain cycling acts either to increase or decrease yield strength depending on material and operating conditions; and temperature acts either to increase or decrease yield strength depending on whether a hardening or softening process occurs in the material at the operating temperature. Thus, the possible inaccuracies prevent this analysis from giving exact values. However, the analysis is still useful in showing strain-cycle trends of the materials used in the EVESR Mark II core.

17.5 NTR Test of EVESR Cladding Materials

Samples of all cladding used for EVESR were sent to VAL for NTR Pile Oscillator Test to determine the boron equivalent.

The calculated and measured boron equivalent absorption is shown in Table 17-4. The calculated values assume the maximum allowable alloying constituents and the highest cross sections.

TABLE 17-4  
NTR TEST OF BORON EQUIVALENT

Material	Sample*	Natural Boron Equivalent Absorption	Natural Boron Equivalent Absorption Calculated from Chemical Analysis
Stainless Steel 304 Type (VM)	2VJ002	790 ±10 ppm	
Stainless Steel 304 Type (Comm.)	Velocity Booster	818 ±10 ppm	
Stainless Steel 304 Type (VM)	2VJ188	791 ±10 ppm	793 ppm
Stainless Steel 304 Type (Comm.)	Process Tube	799 ±10 ppm	
Stainless Steel 304 Type (Comm.)	AVN1014	775 ±10 ppm	767 ppm
Stainless Steel 304 Type (VM)	1VK360	843 ±15 ppm	845 ppm
Incoloy	2VL481	884 ±20 ppm	888 ppm
Incoloy	1VL509	882 ±20 ppm	888 ppm
Inconel	1VM801	1055 ±30 ppm	1062 ppm

\*1 and 2 represent heat numbers.

### 17.6 Heat Transfer Analytical Analysis

A computer program for analysis of multirod superheat fuel element configurations is being developed to perform advanced fuel design calculations. The basic computer logic for this program has been established and computer programming is in progress.

Briefly, this program will permit steady-state heat transfer analysis of seven-rod clusters, taking into account fluid mixing, axial and radial variations in heat generation, as well as the proper temperature for evaluating all material and fluid properties. The comprehensive output includes items such as cladding, steam, and fuel temperatures, in addition to nodal heat losses and pressure drop.

## 18.0 SUB-TASK F-2: FUEL FABRICATION

### 18.1 Fuel Bundle Material Procurement - Mark III

Material orders have been placed with vendors for Zircaloy-2 plate and tubing, and fittings which will be used for the water displacer, process tubes, and downcomers. An order has also been placed for the stainless-steel shield plugs which will be placed inside the risers and downcomers to prevent radiation streaming to the pressure rescue head. The jumper material, including necessary fittings to make the Mark III couplings interchangeable with the current Mark II fuel, has also been ordered. About 90 percent of all material required for the Mark III fuel bundles has now been ordered. The critical exceptions are the Zircaloy "U" fitting for the process tube and the Incoloy "U" fitting for the process tube liner. These items are being given special handling and priority by purchasing to secure a qualified vendor.

The Incoloy tubing required for the Mark III fuel assemblies has been received and processed through incoming receiving inspection. The outside diameter of the tubing is 0.450 inch and the wall thicknesses are 8, 12, 16, and 20 mils.

All tubing has passed incoming inspection except the 8-mil thick material, which was rejected during ultrasonic testing because of scratches on the inside surface of the tubing. The problem has been discussed with the vendor and it was determined that the scratches were a result of processing at the vendor's plant. A replacement order is being initiated to replace the tubing.

The hardware fabrication for the Mark III clusters is 90 percent complete and material for the remaining parts is in the shop.

A purchase order was placed with a vendor in November 1963 to furnish 10 percent enriched  $UO_2$  for the Mark III and Mark IV assemblies. The vendor has been unable to meet the required specifications for the powder and the order was cancelled by default.

Negotiations are now being made with another vendor to supply the powder.

### 18.2 Incoming Tubing Inspections

To insure tubing integrity and to maintain an information file in regard to fuel elements which are to use this tubing, the following tests will be conducted on all incoming Incoloy tubing scheduled for use in Advanced Superheat Experiments.

- a. Macrohardness on smooth surfaces.
- b. Tensile tests at room temperature and at 1100 to 1150 °F.

- c. Hydrostatic testing to rupture.
- d. Chemical analysis, and
- e. Metallography.

The results from these tests should present a well-rounded picture of the mechanical, physical, and metallurgical properties of this material and aid in the eventual post-irradiation examination.

The metallographic examination of the Incoloy-800 seamless tubing made from the special ingot material has been completed and the results are tabulated below.

	ASTM Grain Size	Microhardness		
		2 mils from OD	Center	2 mils from ID
0.450-inch OD by 0.012-inch wall	8-1 2	88.21	84.20	89.62
0.450-inch OD by 0.016-inch wall	8-1 2	85.50	84.20	88.21
0.450-inch OD by 0.020-inch wall	8	76.93	78.07	76.93
0.375-inch OD by 0.016-inch wall	7-1 2	75.81	76.93	78.07
0.280-inch OD by 0.020-inch wall	8-1 2	97.18	85.50	91.07

Some grain boundary precipitation was evident and varied with each tube size. Also evident were stringer-like nonmetallic inclusions in the longitudinal cross sections of all tubing.

## 19.0 SUB-TASK F-3: MARK III FUEL DESIGN

## 19.1 Physics

The present Mark III design calls for four seven-rod clusters per bundle at 10 percent enrichment. These clusters are clad with 8-, 12-, 16-, and 20-mil Incoloy and are contained in an 83-mil-thick Zircaloy process tube. The fuel is physically separated from the process tube by a 28-mil Incoloy liner. Work completed this quarter on this reference design included:

- Gross power distributions across core with "inverse" and "normal" control rod patterns.
- Flooding effects for Mark III in Zone 1, and for Mark III in Zones 1 and 3. (Mark II fuel assumed in the balance of the core.)
- Reactivity worth compared to Mark II.

The maximum heat flux in Mark III fuel with the normal control rod pattern is 55,000 Btu/h-ft<sup>2</sup>. With the inverse rod pattern this number increases to 147,000 Btu/h-ft<sup>2</sup>. These numbers are averages over a seven-rod cluster and do not include an axial factor. A more detailed power picture is being generated which will yield rod-by-rod powers.

Table 19-1 contains flooding coefficients for the core with Mark III fuel in Zone 1 and in Zones 1 and 3. The trend of these numbers indicates that replacing Mark II fuel with Mark III fuel (1) slightly reduces cold unflooding reactivity, (2) increases hot flooding with rods out, and (3) increases the rods out cold-to-hot reactivity swing.

TABLE 19-1  
FLOODING COEFFICIENTS

Control Rods	Event*	Mark III Zone 1	Mark III Zones 1 and 3	Mark II (Startup Core)
All Rods Out	Cold Unflooding	+0.97 percent	+0.91 percent	+1.4 percent
	Hot Flooding	+2.4 percent	+2.6 percent	+2.2 percent
	Cold-to-Hot, Flooded	+4.6 percent	+5.8 percent	+3.6 percent
Stainless Steel Rods In	Hot Flooding	+3.3 percent	+3.1 percent	+2.7 percent
All Rods In	Hot Flooding	+4.2 percent	+3.7 percent	+3.7 percent

\*"Cold unflooding" is with velocity booster (Mark II fuel) and insulation gap flooded (Mark III fuel). "Hot flooding" is complete flooding of the Mark II fuel and insulation gap unflooded in the Mark III fuel.

The Mark III bundles appear to be less reactive than the Mark II bundles. The higher enrichment in Mark III is offset by the smaller amount of UO<sub>2</sub> per bundle and by a higher leakage rate. This leakage is a result of the large amount of Zircaloy present as a water displacer. Table 19-2 below shows the trend of reactivity loss.

TABLE 19-2  
CORE REACTIVITY, NO CORRECTIONS\*

	<u>All Mark II</u>	<u>Mark III Zone 1</u>	<u>Mark III Zones 1 and 3</u>
$k_{\text{eff}}$	1.147	1.138	1.124

\*For shims and miscellaneous neutron absorbers in the core, variable enrichment, or calculation versus measurement corrections.

These numbers indicate approximate differences since corrections which apply to one case do not apply to the other two. A more detailed analysis is being completed which will better determine the absolute reactivity losses.

### 19.2 Heat Transfer and Design Analysis

- a. It was concluded from an analysis of the riser insulation gap that: (1) below the water level a stagnant steam gap is adequate to maintain Zircaloy temperatures which are not excessive, (2) above the water level the riser temperatures are too high for Zircaloy, and (3) the relative expansions between the vessel and the riser tubes is about the same as for the Mark II bundles, thereby preventing excessive stresses at the vessel outlet nozzle. Item (2) makes necessary the use of a joint between the Incoloy riser and the Zircaloy process tubes.
- b. To achieve high specific power in the Mark III fuel, it is desirable to reverse the present control rod pattern; i. e., pull out the four center rods and insert the eight outer ones. This requires a significant safeguards effort to amend the EVESR Operating License in two areas -- changes in control rod pattern, and the maximum specific power allowable within the EVESR core. Work has begun on both items, but to avoid loading delays due to licensing charges it is planned that the Mark III fuel will be inserted in the four center positions with the present EVESR control rod pattern. The rods will then be reversed when the license amendment is obtained.

Based on preliminary calculations the approximate axial peak heat fluxes which can be attained are as follows:

1. Normal rod pattern -- 100,000 Btu/ft<sup>2</sup>/h (13 kw/kg UO<sub>2</sub>)
2. Reversed rod pattern but within current specific power limit for license -- 180,000 Btu/ft<sup>2</sup>/h (23 kw/kg UO<sub>2</sub>)
3. Reversed rod pattern and elimination of specific power limit in license -- 260,000 Btu/ft<sup>2</sup>/h (33 kw/kg UO<sub>2</sub>)

Preliminary calculations of the average moderator voids in the Mark III fuel bundles at 12.5 MWt with the reversed control rod pattern, indicate that voids will not be excessive and circulation should be adequate. These calculations, as well as the similar calculations for the normal rod pattern, will be firmed up following completion of the detailed physics calculations.

Preliminary heat transfer and flow calculations for the entire fuel bundle were made to establish pressure drops and temperatures for mechanical analysis purposes. These calculations were completed for both the normal and reversed control rod patterns.

The pressure drop across the entire bundle configuration, including the jumper, varies from 20 psi with the normal rod pattern to about 250 psi with the reversed rod pattern. The steam flow required per "U" tube is 1500 lb/h and 6000 lb/h, respectively, for the two control rod patterns.

### 19.3 Fuel Bundle Design

The overall layout of the Mark III fuel bundle has been completed and is now undergoing internal review to identify areas requiring major stress, thermal, and safeguard analyses. Following this review, any necessary changes will be made and preparation of detailed drawings will be initiated.

It has been decided that the Incoloy-Zircaloy mechanical joint at the top of the Zircaloy process tubes will be used only between the process tube and riser section and not between the process tube and downcomer section. This joint is not required between the downcomer and process tube, since a Zircaloy downcomer can be used, and any possibility of in-leakage at a location that could affect irradiation results is thereby avoided.

The dissimilar metal mechanical joint, developed under P.A. 13, is being tested by cycling between 125 and 600°F with a 105 psi pressure difference. It revealed no signs of leakage in fifteen cycles, and testing is continuing.

The Mark III bundles will have Inconel jumper adapters, rather than new steam jumpers, to make these bundles compatible with the Mark II jumper arrangement. This will avoid major redesigns should it become necessary to move the Mark III bundles from the four center core positions in the future. Final design of these adapters is proceeding in drafting.

A test unit for determining deflections in the scalloped insulation liner has been completed and preliminary test results obtained. These tests will provide information required to finalize the design with respect to spacers between the liner and process tube and on the operating flow clearance to be expected between the liner and fuel element. The preliminary results appear to be in line with general expectations.

#### 19.4 Bundle Tooling Design and Fabrication

The status of tools for fabrication of the advanced fuel bundles is as follows:

- a. Design of the tooling for outward dimpling of the riser liner is complete.
- b. The liner-process tube joint rolling equipment has been ordered from the supplier.
- c. The scalloping tool for forming the process tube liners has been released to manufacturing, and fabrication is underway. Tubing for sample runs is on order.

#### 19.5 Steam Flow Tests on Advanced Fuel Components

Work has begun on the use of the existing Moss Landing steam facility for flow testing advanced fuel components as well as prototype fuel bundles. Tests will be conducted under steam conditions of 950°F and 1000 psig with steam flows up to 30,000 lb/h.

Preliminary plans call for such tests as pressure drop measurements, check of thermal expansion, vibration, and the effectiveness of thermal insulation schemes, underwater seals, and proof testing overall mechanical designs.

#### 19.6 Mark III Fuel Element Design

The present program calls for four Mark III fuel assemblies. Each assembly will have four seven-rod clusters. The individual rods will be spaced with helical wires and will have 0.450 inch OD Incoloy-800 cladding containing UO<sub>2</sub> pellets of 95 percent of theoretical density. Cladding thickness of 0.020, 0.016, 0.012, and 0.008 inch will be used, with each of the four assemblies utilizing one of the four cladding thicknesses.

Drawings of the Mark III fuel rods and clusters have been issued, as shown in Figures 19-1 and Figure 19-2 (Drawings 107C4473 and 798D810). The center rod of each cluster is pinned to a support rod. The upper end plugs of the outer six rods have grooves which interlock with the support rod. A sleeve fits over the end plugs and support rods to maintain rod axial position. Flats on the end plugs fit against this sleeve to hold angular orientation for proper intermeshing of the wire spacers. At the lower end of the cluster a spacer is pinned to the center rod. The outer rods are free to move axially in the space to accommodate differential expansion.

#### 19.7 Fuel Element Fabrication Development

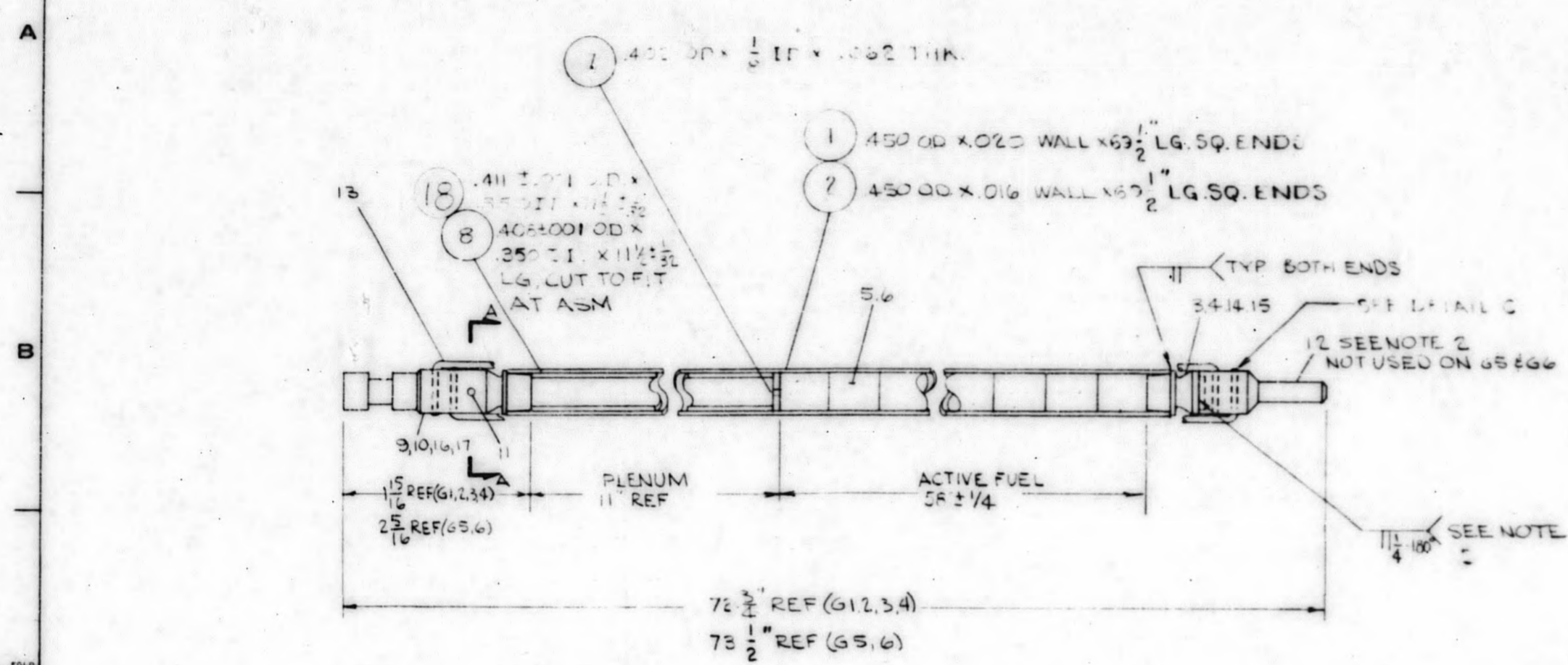
A process flowsheet has been established for fabricating the Mark III fuel clusters. Development work has been initiated to establish details for each fabrication sequence.



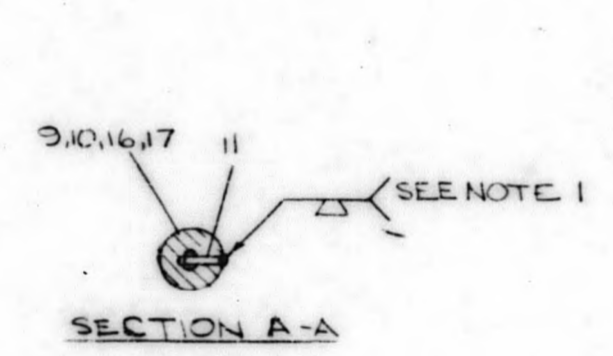
UNLESS OTHERWISE SPECIFIED USE THE FOLLOWING			
APPLIED PRACTICES	SURFACE	TOLERANCES UNLESS OTHERWISE SPECIFIED	FINISH
AS 2.1.1	✓	FRACTIONAL DECIMALS	1000:1

**FUEL ROD**  
FIRST MADE FOR EVESR ADVANCED FUEL  
PL 15 LED

FCF 7051 31



- 1 EACH ROD TO BE OUTGASSED & BACKFILLED WITH HELIUM & MADE SPECTROMETER LEAK TESTED. MAX PERMISSIBLE LEAKAGE TO BE 10<sup>-6</sup> CC/SEC.
- 2 AFTER WELDING WIRES (P13) TO END PLUG (9,10) & PLUG CAP (P12) ROTATE PLUG CAP (P12) SIX TURNS IN 'B' (SEE GRP TAB) DIRECTION & WELD (P12) AS SHOWN. LENGTH OF WIRE (P13) TO BE SUCH THAT ALL SLACK IS REMOVED AFTER SIX ROTATIONS.
- 3 DEPTH OF SURFACE FINISH, WELD BEAD, ETC. AT THE POINT TO BE FILLED 1/8-TENTH OF TUBE WALL THICKNESS.
- 4 BEFORE MAKING FINAL WELD IN G6 # 36 LINE UP 9/64 DIA. HOLE PT. 14 & 15. CAME ANGLE AS 1/8 DIA HOLE IN PT. 10 & 17.



GRPF	'B' (SEE NOTE 2)
G1	RIGHT-HANDED
G2	LEFT-HANDED
G3	RIGHT-HANDED
G4	LEFT-HANDED
G5	NOT APPLICABLE
G6	NOT APPLICABLE

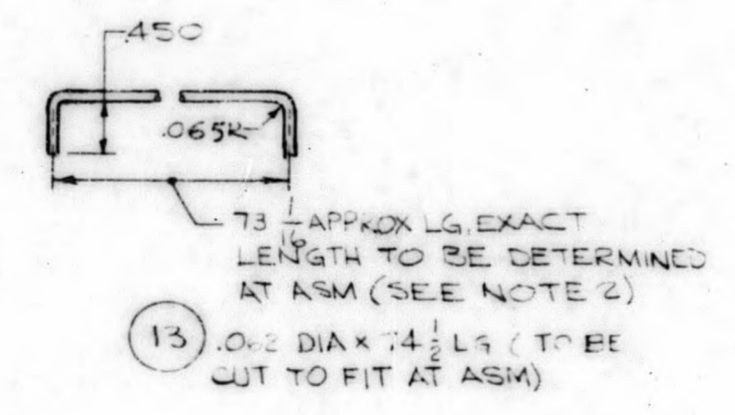
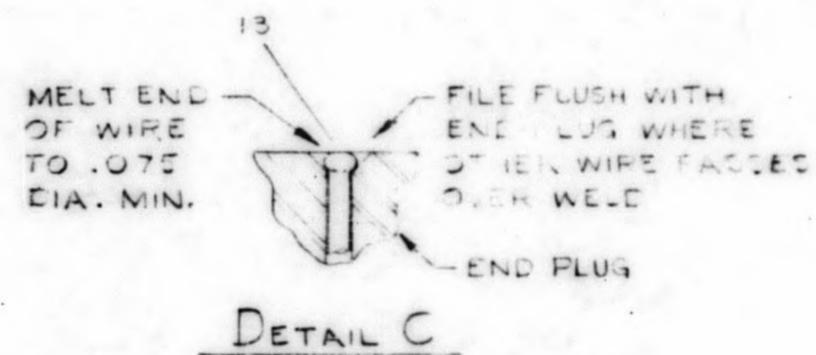
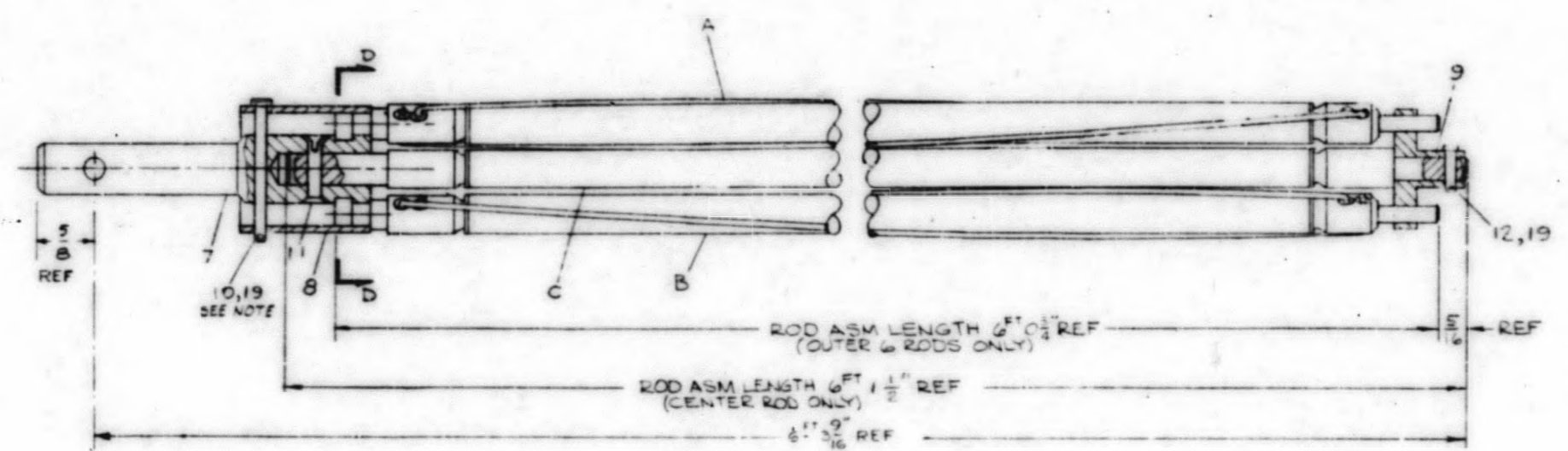
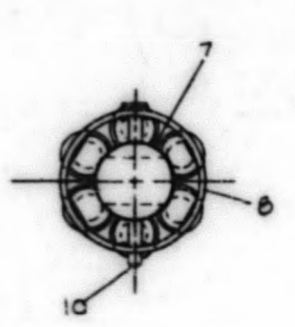


Figure 19-1. EVESR Fuel Rod

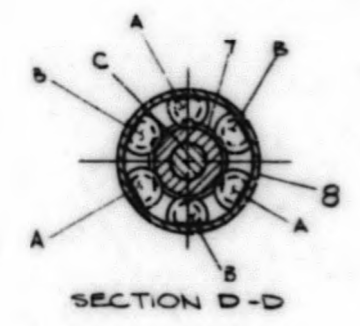
APED	107C4473
SAN - DJE	
JAN 21 '64	

UNLESS OTHERWISE SPECIFIED USE THE FOLLOWING:  
 UNFINISHED SURFACES  
 145A5481

1330810		FUEL CLUSTER MARK III	
FIRST MADE FOR EVESR ADVANCED FUEL			
QTY	PN	NAME	DESCRIPTION
5	1	FUEL ROD	107C4473G1
5	2	FUEL ROD	107C4473G3
3	3	FUEL ROD	107C4473G2
3	4	FUEL ROD	107C4473G4
1	5	FUEL ROD	107C4473G5
1	6	FUEL ROD	107C4473G6
1	7	SUPPORT ROD	159A1614 P1
1	8	SLEEVE	159A1615 P1
1	9	SPACER	159A1616 P1
1	10	PIN	159A1625 P1
1	11	PIN	159A1676 P1
1	12	PIN	159A2006 P1
1	13	FUEL R T	107C4646G6
1	14	FUEL R T	107C4646G4
3	15	FUEL R T	107C4646G1
3	16	FUEL R T	107C4646G2
3	17	FUEL R T	107C4646G3
3	18	FUEL ROD	107C4646G1
ARARAR AR	19	SAFETY WIRE	1057 DIA T.002 IN COLOR ADD FR251931 TYPE 1



	A	B	C
G1	P1	P3	P5
G2	P2	P4	P6
G3	P8	P16	P14
G4	P17	P15	P13



NOTE  
 1. SAFETY WIRE MUST NOT EXTEND OUTWARD MORE THAN  $\frac{1}{8}$  FROM OUTER SURFACE OF P8

Figure 19-2. EVESR Mark III Fuel Cluster

DESCRIPTION OF GROUP	REVISIONS	DATE

APED SAN JOSE  
 JORDAN  
 19-7/19-8  
 JAN 64

### 19.8 Mark III Thermal and Hydraulic-Design Summary

The preliminary thermal and hydraulic characteristics of the Mark III design have been completed and are being reviewed for compatibility with over-all EVFSR system and advanced fuel program requirements. A pictorial cross-section of the Mark III fuel is shown in Figure 19.3. Table 19.3 shows the significant thermal and hydraulic characteristics.

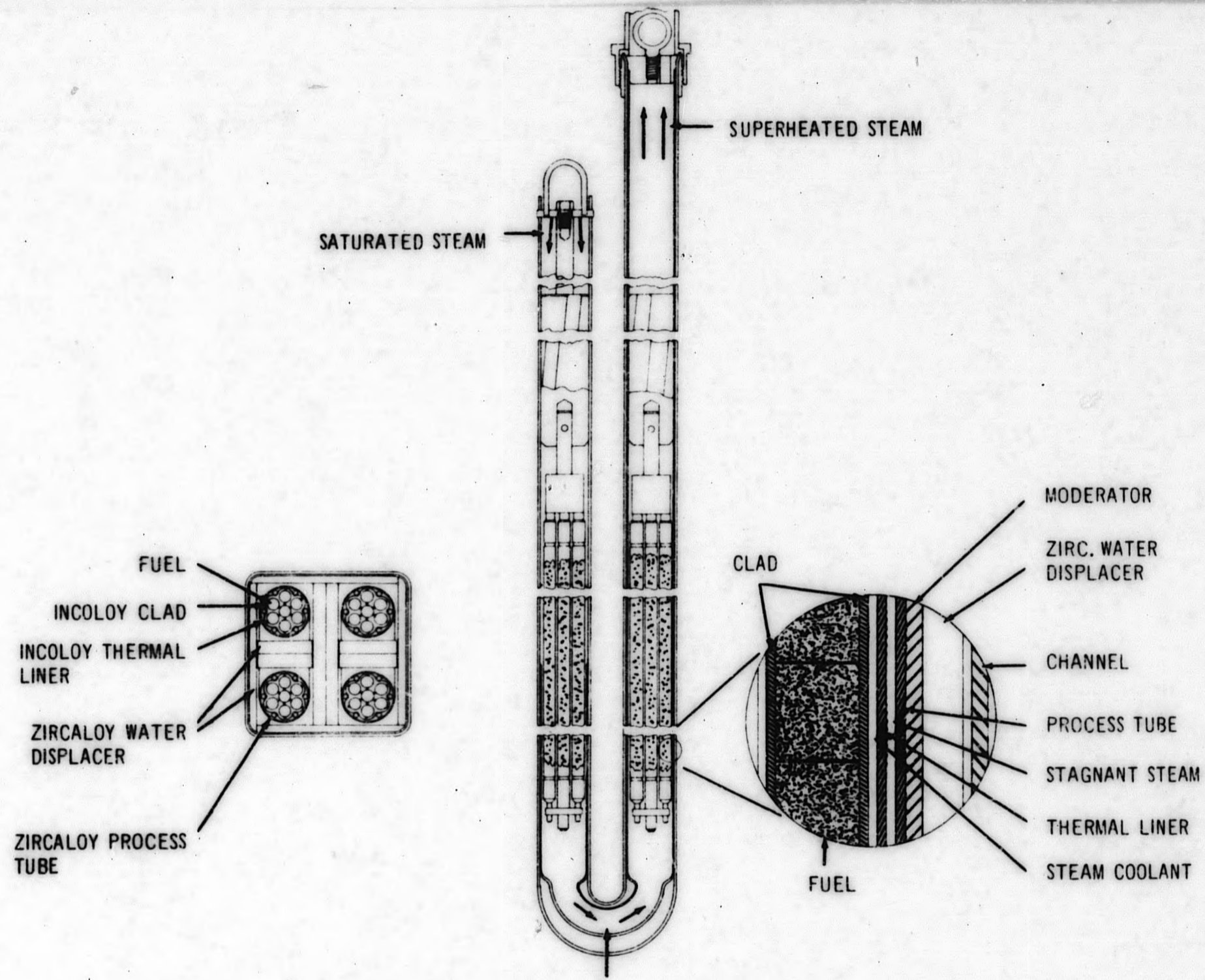


Figure 19.3. Cross Section of EVESR Mark III Fuel

TABLE 19.3  
THERMAL AND HYDRAULIC CHARACTERISTICS OF MARK III FUEL  
AT VARIOUS POWER LEVELS

<u>Fuel Element Data</u>	<u>Power Limited by Use of Normal Control Rod Pattern</u>	<u>Power Limited by 23 kW/kg License Limit</u>	<u>Desired Target Power Conditions</u>
1. Type of fuel element	7-rod Cluster 107C4473 798D810	7-rod Cluster 107C4473 798D810	7-rod Cluster 107C4473 798D810
2. Fuel length, ft-in. 1st pass 2nd pass	5 5	5 5	5 5
3. Rod clad OD, in.	0.45	0.45	0.45
4. Rod clad thickness, in.	0.020	0.020	0.020
5. Rod clad material	Incoloy	Incoloy	Incoloy
6. Fuel spacing method	Wire wrap	Wire wrap	Wire wrap
7. Cluster pitch-to-diameter ratio	1.15	1.15	1.15
8. Type of fuel fabrication	Pellet	Pellet	Pellet
9. Fuel % theoretical density	92	92	92
10. UO <sub>2</sub> /fuel element, Kg	20	20	20
11. Fuel pellet OD, in.	0.422	0.442	0.442
12. Fuel enrichment, %	10	10	10
13. Process tube configuration	1.875 OD Zr tube with 0.030 Incoloy scallop liner	1.875 OD Zr tube with 0.030 Incoloy scallop liner	1.875 OD Zr tube with 0.030 Incoloy scallop liner
14. Process tube insulation	Steam	Steam	Steam
15. Process tube thickness and collapse pressure differential, in; psi	0.083 1300	0.083 1300	0.083 1300
16. Fuel element steam flow area, in <sup>2</sup>	0.60	0.60	0.60
17. Fuel element steam flow area hydraulic diameter, in.	0.139	0.139	0.139
18. Inlet steam temperature, F, 1st pass 2nd pass	545 692	545 696	545 690
19. Inlet steam pressure, psi	1000	1000	1000
20. Axial peaking factor	1.78	1.78	1.78
21. Fuel element power, KW, 1st pass 2nd pass	61.2 66.0	121 121	225.5 225.5

TABLE 19.3 (Continued)

Fuel Element Data (Continued)					
22.	Design steam flow rate, lbs hr	1450	3030	6100	
23.	Design steam exit temp., F	896	891	881	
24.	Average heat flux, Btu hr-ft <sup>2</sup> - F	52,800	100,500	187,300	
25.	Maximum section heat flux, Btu/hr-ft <sup>2</sup> - F	94,000	179,000	333,000	
26.	Maximum peak heat flux, Btu hr-ft <sup>2</sup> - F	106,700	194,000	364,000	
27.	Most probable maximum clad temp., F	1100	1100	1100	
28.	Heat loss to moderator adjacent to fuel region, KW	1st pass	6.7	7.9	8.3
		2nd pass	15.0	18.3	20.2
29.	Fuel element design pressure drop, psi	1st pass	4.5	17.1	61
		2nd pass	5.5	21.4	81
30.	Maximum pressure differential across the insulation liner, psi	10.0	38.5	141	
31.	Bundle pressure drop, psi	19.0	72.0	252	
32.	Heat transfer area per fuel element, ft <sup>2</sup>	1st pass	4.11	4.11	4.11
		2nd pass	4.11	4.11	4.11
33.	Average specific power in fuel element, KW/Kg	6.58	12.52	23.33	
34.	Maximum section specific power in fuel element, KW/Kg	11.71	22.30	41.48	
35.	Maximum steam velocity in fuel element, ft/sec.	73.5	160	372	

Note that the nomenclature "fuel element" refers to the fact that the first and second pass are in series and are considered as one continuous element instead of two discrete sections.

REFERENCES

1. EVESR Final Hazards Summary Report, APED 3958, October 1, 1962.
2. Physics Pre-Startup Report, EVESR, GEAP-4213, April 12, 1963, with Addendum dated August 26, 1963.
3. Honeck, H. C., THERMOS, A Thermalization Transport Theory Code for Reactor Lattice Calculations, BNL-5826, September 1961.
4. EVESR Preliminary Criticals, APED-4204, September 1963.
5. Reynolds, W. C., "Turbulent Heat Transfer in a Circular Tube with Variable Circumferential Heat Flux," *Int. J. Heat Mass Transfer*, 6, 445 (1963).
6. Sutherland, W. A., and Kays, W. M., "Heat Transfer in an Annulus with Variable Circumferential Heat Flux," GEAP-4571, General Electric Co., San Jose, Calif. (1964).
7. Rieger, G. F., "Applications of Strain Cycling Considerations to Superheat Fuel Design," GEAP-4244.
8. Lyons, M. F., et al., "Plastic Strain in Thin Fuel Element Cladding Due to UO<sub>2</sub> Thermal Expansion," GEAP-3739, p. 27.
9. Lyons, M. F., et al., "UO<sub>2</sub> Thermal Conductivity at Elevated Temperatures," *Transactions American Nuclear Society*, Vol. 6, No. 1, June, 1963, p. 152.
10. Burdick, M. D., and Parker, H. S., "Effect of Particle Size on Bulk Density and Strength Properties of Uranium Dioxide Specimens," *J. American Ceramic Society*, Vol. 39, 1956, p. 186.
11. Petersen, G. T., and Weiss, M. L., "Final Physics Report Empire State Atomic Development Associates Vallecitos Experimental Superheat Reactor," APED-4074.



**END**